Weighted Fisher divergence for high-dimensional Gaussian variational inference

Aoxiang Chen, David J. Nott and Linda S. L. Tan

Abstract. Bayesian inference has many advantages for complex models. However, standard Monte Carlo methods for summarizing the posterior can be computationally demanding, and it is attractive to consider optimization-based variational approximations. Our work considers Gaussian approximations with sparse precision matrices which are tractable to optimize in high-dimensional problems. Although the optimal Gaussian approximation is usually defined as the one closest to the target posterior in Kullback-Leibler divergence, it is useful to consider other divergences when the Gaussian assumption is crude, in order to capture important features of the posterior for a given application. Our work studies the weighted Fisher divergence, which focuses on gradient differences between the target posterior and its approximation, with the Fisher and score-based divergences being special cases. We make three main contributions. First, we compare approximations for weighted Fisher divergences under mean-field assumptions for both Gaussian and non-Gaussian targets with Kullback-Leibler approximations. Second, we go beyond mean-field and consider approximations with sparse precision matrices reflecting posterior conditional independence structure for hierarchical models. Using stochastic gradient descent to enforce sparsity, we develop two approaches to minimize the weighted Fisher divergence, based on the reparametrization trick and a batch approximation of the objective. Finally, we examine the performance of our methods for examples involving logistic regression, generalized linear mixed models and stochastic volatility models.

Key words and phrases: Fisher divergence, Score-based divergence, Stochastic gradient descent, Gaussian variational approximation.

Department of Statistics and Data Science, National University of Singapore (e-mail: e0572388@u.nus.edu).
Department of Statistics and Data Science, National University of Singapore (e-mail: standj@nus.edu.sg).
Department of Statistics and Data Science, National University of Singapore (e-mail: statsll@nus.edu.sg).

1. INTRODUCTION

Bayesian inference is a powerful tool for quantifying uncertainty, but it is demanding to implement for two reasons. Firstly, specifying a full probabilistic model for all unknowns and observables requires careful thought, and the components of the model need to be checked against the data. Secondly, Bayesian computations are

difficult, requiring approximation of high-dimensional integrals. For many Bayesian models, exact posterior inference is infeasible, and a variety of numerical methods for summarizing the posterior are used in practice, such as Markov chain Monte Carlo (MCMC) and variational inference (VI). MCMC is asymptotically unbiased, which means that we can estimate posterior quantities as precisely as we wish with a large enough number of iterations. While MCMC is often treated as the gold standard for posterior estimation, its computational cost can be prohibitively high for large datasets or complex models (Robert and Casella, 2004; Maclaurin and Adams, 2015). On the other hand, VI reformulates posterior computation into an optimization problem by minimizing a divergence between the true posterior and a simpler variational distribution. This enables faster and more scalable inference, leveraging advances in optimization algorithms (Blei et al., 2017). As a result, VI is increasingly popular for its computational efficiency in large-scale problems.

The performance of VI is largely determined by the family of variational approximations chosen, optimization technique, and divergence characterizing discrepancy between the true posterior and variational density. Much of the VI literature has focused on improving expressiveness of the variational family and enhancing optimization methods, often using Kullback-Leibler divergence (KLD) as the measure of approximation quality. To better capture the dependence structure among variables, which can be especially strong in hierarchical models, structured variational approximations that mimic the true dependency structure can be employed (Hoffman and Blei, 2015; Tan and Nott, 2018; Durante and Rigon, 2019; Tan, 2021). More recently, flow-based methods which transform an initial simple distribution into more flexible forms through a series of invertible transformations have been introduced (Rezende et al., 2014; Dinh et al., 2017; Agrawal and Domke, 2024). These approaches allow VI to capture highly complex posterior distributions, significantly enhancing the flexibility of the inference.

Despite the popularity of KLD, studying alternatives can be important, particularly when using simple vari-ational families which may be employed for tractability in high-dimensional problems. These approximations may not be capable of matching the target posterior closely, and choosing an appropriate divergence can help to capture the most important features of the posterior for a given application. A family of divergences including KLD as a special case is the Rényi's α family (Li and Turner, 2016), with parameter α that can be adjusted to give Hellinger distance ($\alpha = 0.5$), χ^2-divergence ($\alpha = 2$) and KLD ($\alpha = 1$). The value of α can be chosen to balance between mode-seeking and mass-covering behavior, but when $\alpha \neq 1$, the most practical methods for optimizing the variational Rényi bound use biased stochastic gradients. Stein divergence has also emerged as a powerful objective for VI. Ranganath et al. (2016) introduced operator variational inference, a minimax approach that optimizes Stein discrepancies by constructing variational objectives based on Stein operators. Liu and Wang (2016) developed Stein variational gradient descent, which uses kernelized Stein discrepancies to iteratively transform particles toward the posterior. In this article, we explore use of the weighted Fisher divergence in Gaussian VI, focusing on the Fisher and score-based divergences as special cases. The definitions and motivations for studying these divergences are presented below.

1.1 Weighted Fisher divergence

Let $p(y|\theta)$ be the likelihood of observed data y, where $\theta \in \mathbb{R}^d$ is an unknown model parameter. Consider Bayesian inference with a prior density $p(\theta)$. In classical variational inference (Ormerod and Wand, 2010; Blei et al., 2017), the true posterior $p(\theta|y) = p(y|\theta)p(\theta)/p(y)$ is approximated with a more tractable density $q(\theta)$ by minimizing the KLD between them, where

$$\mathrm{KL}(q\|p) = \int q(\theta) \log \frac{q(\theta)}{p(\theta|y)} d\theta.$$

Let E_q denote expectation with respect to $q(\theta)$. As $\log p(y) = \mathrm{KL}(q\|p) + \mathcal{L}$, where $\mathcal{L} = \mathrm{E}_q\{\log p(y, \theta) - \log q(\theta)\}$, minimizing the KLD is equivalent to maximizing an evidence lower bound $\mathcal{L}$ on $\log p(y)$, which does not depend on the normalizing constant of the true posterior.

Score matching (Hyvärinen, 2005) focuses instead on closeness between gradients of the log densities with respect to the variable θ, although the score function refers conventionally to gradient of the log-likelihood with respect to the parameter. A form of such discrepancy is the weighted Fisher divergence (Barp et al., 2019), defined as

$$S_M(q\|p) = \int q(\theta) \left\| \nabla_\theta \log \frac{q(\theta)}{p(\theta|y)} \right\|_M^2 d\theta$$

$$= E_q\{\|\nabla_\theta \log q(\theta) - \nabla_\theta \log p(\theta|y)\|_M^2\},$$

where $\|\cdot\|_M$ is the M-weighted vector norm defined as $\|z\|_M = \sqrt{z^\top M z}$ and M is a positive semi-definite matrix. Like KLD, $S_M(q\|p)$ is asymmetric, non-negative, and vanishes when $q(\theta) = p(\theta|y)$. Let $h(\theta) = p(y|\theta)p(\theta)$. Then $\nabla_\theta \log p(\theta|y) = \nabla_\theta \log h(\theta)$, which is independent of the unknown normalizing constant $p(y)$. Similarly, if the variational density contains an unknown normalizing constant, this does not need to be computed to evaluate the weighted Fisher divergence. Unlike the evidence lower bound, the weighted Fisher divergence provides a direct measure of the distance between the true posterior and variational density.

When M is the identity matrix I, $S_I(q\|p)$ is known as the *Fisher divergence* (FD, Hyvärinen, 2005), denoted hereafter as $F(q\|p)$. When $q(\theta)$ is $N(\mu, \Sigma)$ and M is its covariance matrix Σ, $S_\Sigma(q\|p)$ is referred to as *score-based divergence* (SD) in Cai et al. (2024), denoted as $S(q\|p)$ henceforth. Cai et al. (2024) derived closed-form updates for Gaussian variational parameters in a batch and match (BaM) algorithm based on score-based divergence, and showed that $S(q\|p)$ is affine invariant while $F(q\|p)$ is not. This means that $S(\tilde{q}\|\tilde{p}) = S(q\|p)$ if $\tilde{p}$ and $\tilde{q}$ denote the densities of p and q respectively after applying an affine transformation of θ.

In recent years, there is increasing interest in use of the weighted Fisher divergence in VI. Huggins et al. (2020) showed that the Fisher divergence defined in terms of the generalized ℓ_p norm is an upper bound to the p-Wasserstein distance, and its optimization ensures closeness of the variational density to the true posterior in terms of important point estimates and uncertainties. Yang et al. (2019) derived an iteratively reweighted least squares algorithm for minimizing the Fisher divergence in exponential family based variational approximations. Elkhalil et al. (2021) employed the factorizable polynomial exponential family as variational approximation in their Fisher autoencoder framework, which has performance competitive with existing ones. Modi et al. (2023) developed Gaussian score matching variational inference with closed form updates, by minimizing the KLD between a target and Gaussian variational density subject to a matching score function constraint. For implicit variational families structured hierarchically, Yu and Zhang (2023) used the Fisher divergence to reformulate the optimization objective into a minimax problem. Cai et al. (2024) proposed a variational family built on orthogonal function expansions, and transformed the optimization objective into a minimum eigenvalue problem using Fisher divergence.

Our contributions in this article are threefold. First, we study behavior of the weighted Fisher divergence in mean-field Gaussian VI for both Gaussian and non-Gaussian targets, showing its tendency to underestimate the posterior variance more severely than KLD. Second, we develop Gaussian VI for high-dimensional hierarchical models where posterior conditional independence structure is captured via a sparse precision matrix. Sparsity is enforced by computing updates using stochastic gradient descent (SGD) and two approaches are proposed for minimizing the weighted Fisher divergence. The first relies on the reparametrization trick (Kingma and Welling, 2014), while the second relies on a biased estimate of the objective based on a batch of samples at each iteration (Elkhalil et al., 2021; Cai et al., 2024). Third, we study the variance of unbiased gradient estimates computed using the reparametrization trick and limiting behavior of the batch approximated weighted Fisher divergence under the mean-field assumption.

This article is organized as follows. We study the quality of posterior mode and variance approximations for Gaussian and non-Gaussian targets in Sections 2 and 3 respectively, when using the weighted Fisher divergence in VI. Section 4 introduces Gaussian VI for hierarchi-

cal models by using a sparse precision matrix to capture posterior conditional independence. Two SGD approaches for minimizing the weighted Fisher divergence are proposed in Sections 5 and 6, based respectively on the reparametrization trick and batch approximation. Experimental results are discussed in Section 7 with applications to logistic regression, generalized linear mixed models (GLMMs) and stochastic volatility models. Section 8 concludes the paper with a discussion of the findings and future work.

2. ORDERING OF DIVERGENCES FOR GAUSSIAN TARGET

Accurate estimation of the posterior variance is important in VI, as it affects uncertainty quantification in Bayesian inference. Here, we establish an ordering of the weighted Fisher and KL divergences according to the estimated posterior variance when the target $p(\theta|y)$ is $N(\nu, \Lambda^{-1})$ with a non-diagonal precision matrix Λ. All divergences considered can recover the true mean ν and precision Λ when the variational family is also Gaussian with a full covariance matrix. However, the computational cost of optimizing a full-rank Gaussian variational approximation can be prohibitive for high-dimensional models. A widely used alternative is the mean-field Gaussian variational approximation, $q(\theta) = N(\mu, \Sigma)$, with a diagonal covariance matrix Σ. The mean-field assumption simplifies the optimization but tends to underestimate the true posterior variance under the KLD (Blei et al., 2017; Tan and Nott, 2018; Giordano et al., 2018). Here, we examine the severity of posterior variance underestimation under the weighted Fisher divergence compared to KLD.

Our results in this section generalize similar results in Margossian et al. (2024) from score-based divergences to the more general class of weighted Fisher divergences. For KLD under the mean-field assumption, Margossian et al. (2024) showed that the posterior mean can be recovered ($\mu = \nu$) and the optimal variance parameter is

$$\Sigma_{ii}^{\text{KL}} = \Lambda_{ii}^{-1} \quad \text{for} \quad i = 1, \dots, d.$$

Thus, the precision is matched by the variational density, but the variance is underestimated. Lemma 1 presents the

weighted Fisher divergence for a general weight matrix M, which is I_d in the Fisher divergence and Σ in the score-based divergence.

LEMMA 1. *The M-weighted Fisher divergence between a Gaussian target $p(\theta|y) = N(\theta|\nu, \Lambda^{-1})$ and Gaussian variational approximation $q(\theta) = N(\theta|\mu, \Sigma)$ is*

$$S_M(q\|p) = \text{tr}(\Sigma^{-1}M) + \text{tr}(\Lambda M \Lambda \Sigma) - 2\text{tr}(M\Lambda)$$
$$+ (\mu - \nu)^\top \Lambda M \Lambda (\mu - \nu).$$

If Σ is a diagonal matrix, then

$$S_M(q\|p) = \sum_{i=1}^d \{\Sigma_{ii}^{-1}M_{ii} + (\Lambda M \Lambda)_{ii}\Sigma_{ii}\} - 2\text{tr}(M\Lambda)$$
$$+ (\mu - \nu)^\top \Lambda M \Lambda (\mu - \nu).$$

PROOF. The M-weighted Fisher divergence is

$$S_M(q\|p) = \text{E}_q\{\|\nabla_\theta \log q(\theta) - \nabla_\theta \log p(\theta|y)\|_M^2\}$$
$$= \text{E}_q\{\|\Sigma^{-1}(\theta - \mu) - \Lambda(\theta - \nu)\|_M^2\}$$
$$= \text{E}_q\{\|(\Sigma^{-1} - \Lambda)(\theta - \mu) - \Lambda(\mu - \nu)\|_M^2\}$$
$$= \text{tr}\{(\Sigma^{-1} - \Lambda)M(\Sigma^{-1} - \Lambda)\Sigma\}$$
$$+ (\mu - \nu)^\top \Lambda M \Lambda (\mu - \nu)$$
$$= \text{tr}(\Sigma^{-1}M) + \text{tr}(\Lambda M \Lambda \Sigma) - 2\text{tr}(M\Lambda)$$
$$+ (\mu - \nu)^\top \Lambda M \Lambda (\mu - \nu).$$

The final result arises from $\text{tr}(AB) = \sum_{i=1}^d A_{ii}B_{ii}$ if A is a diagonal matrix. □

From Lemma 1, $\nabla_\mu S_M(q\|p) = 2\Lambda M \Lambda(\mu - \nu)$. Thus, $\nabla_\mu S_M(q\|p) = 0$ implies $\mu = \nu$, and the true posterior mean is recovered for any M-weighted Fisher divergence where M is independent of μ. Under the mean-field assumption, at this optimal value of μ,

$$S_M(q\|p) = \sum_{i=1}^d \{\Sigma_{ii}^{-1}M_{ii} + (\Lambda M \Lambda)_{ii}\Sigma_{ii}\} - 2\text{tr}(M\Lambda).$$

If the weight M is independent of Σ, then $\nabla_{\Sigma_{ii}}S_M(q\|p) = (\Lambda M \Lambda)_{ii} - M_{ii}/\Sigma_{ii}^2 = 0$ implies

$$\Sigma_{ii} = \sqrt{M_{ii}/(\Lambda M \Lambda)_{ii}} \quad \text{for} \quad i = 1, \dots, d.$$

4

Thus a closed form solution exists for any M independent of Σ. Moreover, if M is a diagonal matrix, then

$$(1) \qquad \Sigma_{ii} = \sqrt{\frac{M_{ii}}{\sum_{j=1}^{d} M_{jj} \Lambda_{ij}^2}} \quad \text{for} \quad i = 1, \ldots, d.$$

When $M_{ii} = 1 \, \forall \, i$, we recover the Fisher divergence for which the optimal variance parameters are

$$(2) \qquad \Sigma_{ii}^{\text{F}} = \frac{1}{\sqrt{\sum_{j=1}^{d} \Lambda_{ij}^2}} \quad \text{for} \quad i = 1, \ldots, d.$$

Optimal variational parameters for score-based divergence under mean-field assumption have been presented in Margossian et al. (2024), and a discussion is included here for completeness. Plugging $M = \Sigma$ in Lemma 1,

$$S(q\|p) = d + \sum_{i=1}^{d} \sum_{j=1}^{d} \Sigma_{ii} \Sigma_{jj} \Lambda_{ij}^2 - 2 \sum_{i=1}^{d} \Sigma_{ii} \Lambda_{ii},$$

at the optimal value of μ. Let $\mathbf{s} = (s_1, \ldots, s_d)^\top$ such that $s_i = \Sigma_{ii} \Lambda_{ii} \geq 0$, and H be a $d \times d$ symmetric matrix with $H_{ij} = \Lambda_{ij}^2 / (\Lambda_{ii} \Lambda_{jj})$. Then $S(q\|p) = d + 2F(\mathbf{s})$, where

$$(3) \qquad F(\mathbf{s}) = \frac{1}{2} \mathbf{s}^\top H \mathbf{s} - \mathbf{1}^\top \mathbf{s}.$$

Thus the optimal Σ_{ii}^{S} that minimizes $S(q\|p)$ can be obtained by solving a non-negative quadratic program (NQP) for $\mathbf{s}$. NQP is the problem of minimizing the quadratic objective function in (3) subject to the constraint $s_i \geq 0 \, \forall \, i$. Since Λ is positive definite,

$$x^\top H x = \sum_{i=1}^{d} \sum_{j=1}^{d} (x_i/\Lambda_{ii}) \Lambda_{ij}^2 (x_j/\Lambda_{jj}) = y^\top \Lambda y > 0$$

for any $x = (x_1, \ldots, x_d)^\top \in \mathbb{R}^d$ and $y = (x_1/\Lambda_{11}, \ldots, x_d/\Lambda_{dd})^\top$. Thus H is symmetric positive definite, which implies that $F(\mathbf{s})$ is bounded below and its optimization is convex. However, there is no analytic solution for the global minimum due to the non-negativity constraints and iterative solutions are required (Sha et al., 2003). The Karush-Kuhn-Tucker (KKT) conditions are first derivative tests that can be used to check whether a solution returned by an iterative solver is indeed a local optimum. For the NQP in (3), the KKT conditions state that $\forall \, i = 1, \ldots, d$, either (a) $s_i = 0$ and $(H\mathbf{s})_i > 1$ or (b) $s_i > 0$ and $(H\mathbf{s})_i = 1$. Note that $\nabla_{\mathbf{s}} F(\mathbf{s}) = H\mathbf{s} - \mathbf{1}$. These conditions correspond to cases

where the constraint is active or inactive at the optimum. Case (a) implies $\Sigma_{ii}^{\text{S}} = 0$, meaning that the variational density collapses to a point estimate in the ith dimension. Note that the KL and Fisher divergences do not face this issue of "variational collapse". Case (b) implies

$$(4) \qquad \begin{aligned} (H\mathbf{s})_i &= \sum_{j=1}^{d} H_{ij} s_j = \sum_{j=1}^{d} \frac{\Lambda_{ij}^2}{\Lambda_{ii} \Lambda_{jj}} \Sigma_{jj} \Lambda_{jj} = 1 \\ &\implies \sum_{j=1}^{d} \Lambda_{ij}^2 \Sigma_{jj} = \Lambda_{ii}. \end{aligned}$$

Next, we investigate how the variance parameters $\{\Sigma_{ii}\}$ obtained by minimizing the weighted Fisher divergence compare to those obtained by minimizing the KLD.

THEOREM 1. *Suppose the target is a multivariate Gaussian with non-diagonal precision matrix Λ, and the variational family is Gaussian with diagonal covariance matrix Σ. Let Σ_{ii}^{KL}, Σ_{ii}^{M} and Σ_{ii}^{S} denote the optimal value of the ith diagonal element of Σ obtained by minimizing the KL, M-weighted Fisher and score-based divergences respectively, where M is a positive definite diagonal matrix independent of Σ. Then*

$$\Sigma_{ii}^{M} \leq \Sigma_{ii}^{KL} \quad \text{and} \quad \Sigma_{ii}^{S} \leq \Sigma_{ii}^{KL} \quad \text{for} \quad i = 1, \ldots, d.$$

Moreover, $\exists i \in \{1, \ldots, d\}$ such that $\Sigma_{ii}^{M} < \Sigma_{ii}^{KL}$ and $\Sigma_{ii}^{S} < \Sigma_{ii}^{KL}$.

PROOF. We first prove $\Sigma_{ii}^{\text{M}} \leq \Sigma_{ii}^{\text{KL}} \, \forall i$. From (1),

$$(5) \quad \Sigma_{ii}^{\text{M}} = \sqrt{\frac{M_{ii}}{\sum_{j=1}^{d} M_{jj} \Lambda_{ij}^2}} \leq \sqrt{\frac{M_{ii}}{M_{ii} \Lambda_{ii}^2}} = \frac{1}{\Lambda_{ii}} = \Sigma_{ii}^{\text{KL}}.$$

Since Λ has at least one nonzero off-diagonal entry, $\exists i \in \{1, \ldots, d\}$ such that the inequality in (5) is strict. The proof for $\Sigma_{ii}^{\text{S}} \leq \Sigma_{ii}^{\text{KL}}$ is given in Margossian et al. (2024) and we include it here for entirety. From the KKT conditions discussed earlier, if case (a) applies, then $\Sigma_{ii}^{\text{S}} = 0 < \Sigma_{ii}^{\text{KL}}$. Otherwise, case (b) applies and (4) implies that

$$(6) \quad \Lambda_{ii}^2 \Sigma_{ii}^{\text{S}} \leq \sum_{j} \Lambda_{ij}^2 \Sigma_{ii}^{\text{S}} = \Lambda_{ii} \implies \Sigma_{ii}^{\text{S}} \leq \frac{1}{\Lambda_{ii}} = \Sigma_{ii}^{\text{KL}}.$$

To obtain the strict inequality, note that if case (a) applies for at least one i, then $\Sigma_{ii}^{S} < \Sigma_{ii}^{KL}$ for such an i. Otherwise, case (b) applies $\forall \, i$. Since Λ has at least one nonzero off-diagonal
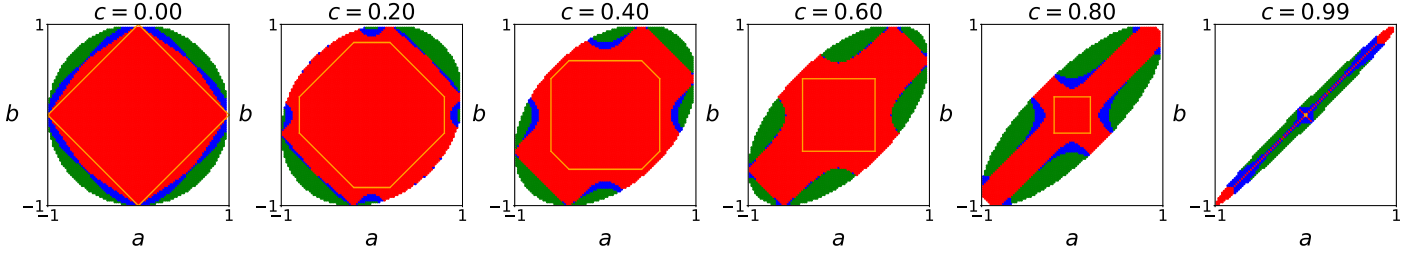
Fig 1: Variance parameter comparisons for Fisher and score-based divergence.

off-diagonal entry, $\exists\, i \in \{1,\dots,d\}$ such that the first inequality in (6) is strict. $\qquad\square$

From Theorem 1, both the weighted Fisher and score-based divergences tend to underestimate the posterior variance more severely than KLD under the mean-field assumption, but ordering between the Fisher and score-based divergences is more nuanced. If case (a) of the KKT conditions apply, then $\Sigma_{ii}^{\mathrm{S}} = 0 < \Sigma_{ii}^{\mathrm{F}}$. If case (b) applies, then from (2) and (4),

$$\Lambda_{ii}^2 \Sigma_{ii}^{\mathrm{S}} \leq \sum_{j=1}^d \Lambda_{ij}^2 \Sigma_{jj}^{\mathrm{S}} = \Lambda_{ii}\Sigma_{ii}^{\mathrm{F}}\sqrt{\sum_{j=1}^d \Lambda_{ij}^2}$$

$$\implies \Sigma_{ii}^{\mathrm{S}} \leq \Sigma_{ii}^{\mathrm{F}}\frac{\sqrt{\sum_{j=1}^d \Lambda_{ij}^2}}{\Lambda_{ii}}.$$

Moreover, if Λ is a *diagonally dominant* matrix such that $\sum_{j\neq i}|\Lambda_{ij}| \leq |\Lambda_{ii}|\;\forall\, i$, then

$$\Sigma_{ii}^{\mathrm{S}} \leq \Sigma_{ii}^{\mathrm{F}}\frac{\sqrt{\Lambda_{ii}^2 + \sum_{j\neq i}\Lambda_{ij}^2}}{\Lambda_{ii}} \leq \Sigma_{ii}^{\mathrm{F}}\frac{\sqrt{\Lambda_{ii}^2 + (\sum_{j\neq i}|\Lambda_{ij}|)^2}}{\Lambda_{ii}}$$

$$\leq \Sigma_{ii}^{\mathrm{F}}\frac{\sqrt{\Lambda_{ii}^2 + \Lambda_{ii}^2}}{\Lambda_{ii}} = \sqrt{2}\Sigma_{ii}^{\mathrm{F}}.$$

Thus the ratio of $\Sigma_{ii}^{\mathrm{S}}/\Sigma_{ii}^{\mathrm{F}}$ is bounded by $\sqrt{2}\;\forall\, i$ if Λ is diagonally dominant.

For a more concrete comparison of posterior variance approximation based on Fisher and score-based divergences, consider a three-dimensional Gaussian target with precision matrix,

$$\Lambda = \begin{bmatrix} 1 & a & b \\ a & 1 & c \\ b & c & 1 \end{bmatrix}.$$

For Fisher divergence, Σ_{ii}^{F} can be obtained from (2), while the splitting conic solver (SCS, O'Donoghue et al.,

2016) in the CVXPY Python package is used to solve the NQP in (3) for score-based divergence. SCS is designed for convex optimization problems characterized by conic constraints, such as nonnegative constraints. It decomposes the optimization task into smaller subproblems solved iteratively by operator-splitting techniques.

Fig 1 illustrates how variance parameters obtained from the Fisher and score-based divergences compare by varying the conditional correlations a, b and c, with each plot representing a value of c. The colored regions represent configurations for which Λ is positive definite. The red, blue and green regions indicate where $\Sigma_{ii}^S \leq \Sigma_{ii}^F$ for all cases, only two cases and only one case respectively. There is no region such that $\Sigma_{ii}^S > \Sigma_{ii}^F\;\forall\, i$. Variance estimates based on score-based divergence have a higher tendency to exceed those based on Fisher divergence when the conditional correlation a, b or c has a large magnitude. The orange-bordered region indicates where Λ is diagonally dominant, and $\Sigma_{ii}^{\mathrm{S}}/\Sigma_{ii}^{\mathrm{F}}$ can be bounded even more tightly by 1 instead of only $\sqrt{2}$ in this example.

3. ORDERING OF DIVERGENCES FOR NON-GAUSSIAN TARGET

Next, we study ordering of the Fisher, score-based and KL divergences in posterior mode and variance estimation when the target $p(\theta|y)$ is a univariate non-Gaussian density, while the variational density $q(\theta)$ is $\mathrm{N}(\mu,\sigma^2)$ with mean $\mu \in \mathbb{R}$ and standard deviation $\sigma > 0$. In the examples below, the VI objective function is available in closed form or can be computed numerically, and optimal variational approximations are obtained using L-BFGS via the `optim` function in R. For univariate densities,
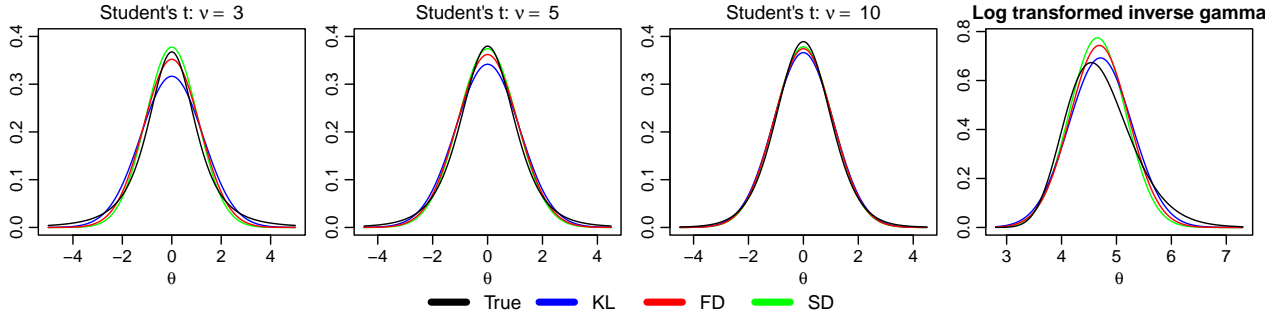
Fig 2: Gaussian variational approximations for Student's t and log transformed inverse gamma.

$S(q\|p) = \sigma^2 F(q\|p)$, so we only present the Fisher divergence. All derivations are given in the supplement.

Let m_* and σ_*^2 denote the mode and variance of the target density. To evaluate the performance of different divergences, we use three criteria, normalized absolute difference in mode: $|\mu - m_*|/\sigma_*$, variance ratio: σ^2/σ_*^2, and integrated absolute error : $\mathrm{IAE}(q) = \int |q(\theta) - p(\theta|y)| d\theta$, which is invariant under monotone transformations of θ and lies in $[0, 2]$. We define $\mathrm{Accuracy}(q) = 1 - \mathrm{IAE}(q)/2$, where a higher accuracy indicates a better approximation of the target.

3.1 Student's t

First, we consider the univariate Student's t as target, which is symmetric but has heavier tails than a Gaussian. The probability density function (pdf) for $\theta \sim t(\nu)$ is $p(\theta|y) = \left(1 + \theta^2/\nu\right)^{-(\nu+1)/2} \Gamma(\frac{\nu+1}{2})/(\sqrt{\pi\nu}\,\Gamma(\frac{\nu}{2}))$, where $\nu \in \{3, 5, 10\}$ is the degrees of freedom. For KLD, we maximize the lower bound,

$$\mathcal{L} = \log\left\{\Gamma\left(\frac{\nu+1}{2}\right)\right\} - \frac{1}{2}\log\left\{\Gamma^2\left(\frac{\nu}{2}\right)\nu\right\}$$
$$- \frac{\nu+1}{2}\mathrm{E}_q\log\left(1 + \frac{\theta^2}{\nu}\right) + \frac{1}{2}\log(2\sigma^2) + \frac{1}{2}.$$

The Fisher divergence is

$$F(q\|p) = (\nu+1)^2 \mathrm{E}_q\left\{\frac{\theta^2}{(\nu+\theta^2)^2}\right\} + \frac{1}{\sigma^2}$$
$$- \frac{2(\nu+1)}{\sigma^2}\mathrm{E}_q\left\{\frac{\theta(\theta-\mu)}{\nu+\theta^2}\right\}.$$

All three divergences successfully capture the mode of the target at 0. From Table 1, SD exhibits the most posterior variance underestimation, followed by FD, while KLD has the least underestimation. In terms of the IAE,

	σ^2/σ_*^2			accuracy		
ν	KLD	FD	SD	KLD	FD	SD
3	0.529	0.428	0.372	92.18	93.66	92.62
5	0.818	0.728	0.681	94.72	95.82	95.97
10	0.950	0.909	0.889	97.01	97.55	97.73

TABLE 1
Variance ratio and accuracy for Student's t.

both FD and SD yield approximations with higher accuracy than KLD. Fig 2 (first 3 plots) compares variational densities with the target. KLD tends to underestimate the probability mass around the mode more severely than FD and SD.

3.2 Log transformed inverse-gamma

Next, consider the normal sample model in Tan and Chen (2024), where $y_i|\theta \sim \mathrm{N}(0, \exp(\theta))$ for $i = 1, \ldots, n$, with prior $\exp(\theta) \sim \mathrm{IG}(a_0, b_0)$ and $a_0 = b_0 = 0.01$. The true posterior of $\exp(\theta)$ is $\mathrm{IG}(a_1, b_1)$, where $a_1 = a_0 + n/2$ and $b_1 = b_0 + \sum_{i=1}^n y_i^2/2$. We simulate $n = 6$ observations by setting $\exp(\theta) = 225$. The lower bound for minimizing the KLD is

$$\mathcal{L} = \frac{1-n}{2}\log(2\pi) + a_0 \log b_0 - \log\Gamma(a_0) - a_1\mu$$
$$- \exp\left(\frac{\sigma^2 - 2\mu}{2}\right)T + \frac{1}{2}\log(\sigma^2) + \frac{1}{2}.$$

The Fisher divergence is

$$F(q\|p) = a_1^2 + b_1^2 \exp\left(2\sigma^2 - 2\mu\right)$$
$$- 2b_1(a_1+1)\exp(\sigma^2/2 - \mu) + 1/\sigma^2.$$

Table 3 shows that SD provides the most accurate mode approximation but also exhibits the most severe variance underestimation. On the other hand, KLD yields the least
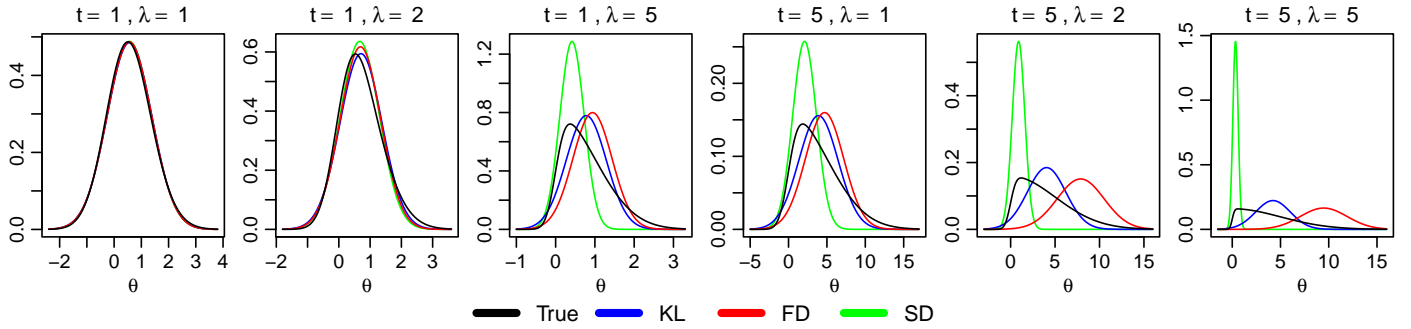
Fig 3: Gaussian variational approximations for skew normal.

(t, λ)	$|\mu - m_*|/\sigma_*$			σ^2/σ_*^2			accuracy		
	KLD	FD	SD	KLD	FD	SD	KLD	FD	SD
(1, 1)	0.07	0.07	0.07	0.992	0.984	0.979	98.27	98.31	98.32
(1, 2)	0.25	0.23	0.20	0.919	0.851	0.803	93.77	93.81	93.79
(1, 5)	0.66	0.91	0.07	0.677	0.642	0.248	83.93	76.44	68.50
(5, 1)	0.66	0.91	0.07	0.677	0.642	0.248	83.92	76.42	68.49
(5, 2)	0.94	2.20	0.10	0.504	0.757	0.054	76.50	45.38	37.06
(5, 5)	1.20	2.94	0.09	0.352	0.644	0.008	68.00	30.35	16.35

TABLE 2

Results of KL, Fisher and score-based divergences for skew normal.

accurate mode approximation while most closely matching the target variance. Overall, KLD has the highest accuracy followed by FD and SD. A visualization is given in Fig 2 (last plot).

	KLD	FD	SD
$|\mu - m_*|/\sigma_*$	0.26	0.23	0.18
σ^2/σ_*^2	0.845	0.732	0.674
accuracy	92.67	91.91	91.53

TABLE 3

Results for log transformed inverse-gamma.

3.3 Skew normal

Finally, let the target be a univariate skew normal. The pdf of $\theta \sim \mathrm{SN}(m, t, \lambda)$ is $p(\theta|y) = 2\,\phi(\theta|m, t^2)\,\Phi\{\lambda(\theta - m)\}$, where $m \in \mathbb{R}$, $t > 0$ and $\lambda \in \mathbb{R}$ are the location, scale and skewness parameters respectively, and $\Phi(\cdot)$ is cumulative distribution function (cdf) of the standard normal. For KLD, we maximize the lower bound,

$$\mathcal{L} = \log 2 - \log(t) - \frac{\sigma^2 + (\mu - m)^2}{2t^2}$$

$$+ \mathrm{E}_q \log[\Phi\{\lambda(\theta - m)\}] + \log(\sigma) + \frac{1}{2}.$$

The Fisher divergence is

$$F(q\|p) = \frac{\sigma^2 + (\mu - m)^2}{t^4} + \lambda^2 \mathrm{E}_q \left[\frac{\phi^2\{\lambda(\theta - m)\}}{\Phi^2\{\lambda(\theta - m)\}}\right]$$

$$- \frac{2\lambda}{t^2} \mathrm{E}_q \left[(\theta - m)\frac{\phi\{\lambda(\theta - m)\}}{\Phi\{\lambda(\theta - m)\}}\right] - \frac{2}{t^2}$$

$$+ \frac{2\lambda}{\sigma^2} \mathrm{E}_q \left[(\theta - \mu)\frac{\phi\{\lambda(\theta - m)\}}{\Phi\{\lambda(\theta - m)\}}\right] + \frac{1}{\sigma^2}.$$

We set $m = 0$ and let $t \in \{1, 5\}$ and $\lambda \in \{1, 2, 5\}$. From Table 2, SD captured the mode most accurately across all settings, followed by KLD and FD (for which estimation of the mode is very poor when both scale and skewness are large). All three divergences underestimated the variance, with KLD and FD exhibiting less underestimation than SD (for which the variance estimate approaches zero as t and λ increase). The accuracies of FD and SD are very close to KLD when $t = 1$ and $\lambda \in \{1, 2\}$. However, KLD has higher accuracy than both FD and SD as skewness and scale increase. Fig 3 shows density plots of the target and optimal variational approximations. SD is good at identifying the mode, whereas FD and KLD estimate

the variance more accurately. Multiple local minimums were detected for the SD in this context.

The examples in this section suggest that SD captures the mode more accurately than FD and KLD if the target density is skewed, but underestimates the posterior variance most severely. KLD has higher accuracy than both FD and SD when the target is skewed, but lower accuracy when the target is symmetric and has heavy tails.

4. SPARSE GAUSSIAN VARIATIONAL APPROXIMATIONS

Next, we consider Gaussian VI for hierarchical models and compare performances of the Fisher, score-based and KL divergences. Given observed data $y = (y_1, \ldots, y_n)^\top$, the variable $\theta = (\theta_L^\top, \theta_G^\top)^\top \in \mathbb{R}^d$ of a two-tier hierarchical model can be partitioned into a *global* variable θ_G that is shared among all observations and *local* variables $\theta_L = (b_1^\top, \ldots, b_n^\top)^\top$, where b_i is specific to the observation y_i for $i = 1, \ldots, n$. Let the joint likelihood of the model be

$$(7) \quad p(y, \theta) = p(\theta_G) p(b_1, \ldots, b_\ell | \theta_G) \times$$

$$\prod_{k=\ell+1}^{n} p(b_k | b_{k-1}, \ldots, b_{k-\ell}, \theta_G) \prod_{i=1}^{n} p(y_i | \theta_G, b_i),$$

where $\{y_i\}$ are conditionally independent given θ, and the $\{b_i\}$ follow an ℓth order Markov model given θ_G. Thus $\{b_i\}$ are conditionally independent of each other a posteriori given the ℓ neighboring values and θ_G. In a random effects model, $\{b_i\}$ are the random effects with $\ell = 0$, while for a state space model, $\{b_i\}$ are the latent states with $\ell = 1$.

Let $q_\lambda(\theta)$ be $N(\mu, \Sigma)$, a Gaussian variational approximation of the posterior density with mean $\mu \in \mathbb{R}^d$ and covariance matrix $\Sigma \in \mathbb{R}^{d \times d}$. Consider a Cholesky decomposition of the precision matrix $\Omega = \Sigma^{-1} = TT^\top$ where T is a lower triangular matrix, and denote the variational parameters as $\lambda = (\mu^\top, \text{vech}(T)^\top)^\top$, where $\text{vech}(\cdot)$ is an operator that stacks lower triangular elements of a matrix columnwise from left to right into a vector.

In a multivariate Gaussian, conditional independence implies sparse structure in the precision matrix, with $\Omega_{ij} = 0$ if θ_i and θ_j are conditionally independent given

the remaining variables. By Proposition 1 of Rothman et al. (2010), Cholesky factor T has the same row-banded structure as Ω. Suppose T is block partitioned according to $(b_1^\top, \ldots, b_n^\top, \theta_G^\top)^\top$, with corresponding blocks T_{ij} for $i, j = 1, \ldots, n+1$. If $T_{ij} = 0$ for $1 \le j \le i - l$ and $j > i$ (as T is lower-triangular), then Ω reflects the conditional independence structure of the true posterior. When θ is high-dimensional, exploiting the conditional independence structure in the model is essential to making Gaussian VI feasible, as the number of parameters to be optimized in T grows quadratically with n. However, after imposing sparsity on T, the number of parameters only grows linearly with n.

We propose two SGD approaches for minimizing the Fisher and score-based divergences, as SGD allows updating of only the elements in T that are not constrained to zero by sparsity. Algorithms that minimize the FD and SD based on unbiased gradient estimates derived using the reparametrization trick are named FDr and SDr ("r" for reparametrization trick, see Table 4), while algorithms that rely on a batch approximation of the FD and SD are named FDb and SDb ("b" for batch approximation, see Table 5) respectively.

5. SGD BASED ON REPARAMETERIZATION TRICK

The Fisher and score-based divergences between $q_\lambda(\theta)$ and $p(\theta|y)$ can be written as

$$F(\lambda) = \mathrm{E}_q[g(\lambda, \theta)^\top g(\lambda, \theta)],$$

$$S(\lambda) = \mathrm{E}_q[f(\lambda, \theta)^\top f(\lambda, \theta)],$$

respectively, where $g(\lambda, \theta) = \nabla_\theta \log h(\theta) - \nabla_\theta \log q_\lambda(\theta)$, $f(\lambda, \theta) = T^{-1} g(\lambda, \theta)$ and $h(\theta) = p(\theta)p(y|\theta)$ as defined previously. We derive gradients of the Fisher and score-based divergences by applying the reparametrization trick of Kingma and Welling (2014). Instead of simulating θ directly from $q_\lambda(\theta)$, we generate $z \sim N(0, I_d)$ and compute $\theta = \mu + T^{-\top} z$. Thus

$$F(\lambda) = \mathrm{E}_\phi \left\{ g(\lambda, \mu + T^{-\top} z)^\top g(\lambda, \mu + T^{-\top} z) \right\},$$

$$S(\lambda) = \mathrm{E}_\phi \left\{ f(\lambda, \mu + T^{-\top} z)^\top f(\lambda, \mu + T^{-\top} z) \right\},$$

where $E_\phi(\cdot)$ denotes expectation with respect to $\phi(z)$, the pdf of $N(0, I_d)$. Note that

$$g(\lambda, \theta) = \nabla_\theta \log h(\theta) + TT^\top(\theta - \mu),$$

$$f(\lambda, \theta) = T^{-1}\nabla_\theta \log h(\theta) + T^\top(\theta - \mu),$$

both of which depends on λ directly as well as through θ. Applying the chain rule,

$$\nabla_\mu F(\lambda) = 2E_\phi\{\nabla_\theta^2 \log h(\theta) g(\lambda, \theta)\},$$

$$\nabla_\mu S(\lambda) = 2E_\phi\{\nabla_\theta^2 \log h(\theta)\Sigma g(\lambda, \theta)\},$$

$$\nabla_{\text{vech}(T)} F(\lambda) = 2E_\phi \text{vech}\Big\{g(\lambda, \theta)z^\top$$
$$- T^{-\top}zg(\lambda, \theta)^\top \nabla_\theta^2 \log h(\theta) T^{-\top}\Big\},$$

$$\nabla_{\text{vech}(T)} S(\lambda) = -2E_\phi \text{vech}\Big\{\Sigma g(\lambda, \theta)\nabla_\theta \log h(\theta)^\top T^{-\top}$$
$$+ T^{-\top}zg(\lambda, \theta)^\top \Sigma \nabla_\theta^2 \log h(\theta) T^{-\top}\Big\}.$$

Detailed derivations are given in the supplement.

Unbiased estimates of the gradients can be obtained by sampling from $\phi(z)$. All gradient computations can be done efficiently even in high-dimensions, as they only involve sparse matrix multiplications and solutions of sparse triangular linear systems. The Hessian $\nabla_\theta^2 \log h(\theta)$ has the same block sparse structure as Ω, as b_i and b_j only occur in the same factor of (7) if b_j is one of the ℓ neighboring values of b_i. For $\nabla_{\text{vech}(T)} F(\lambda)$ and $\nabla_{\text{vech}(T)} S(\lambda)$, we only need to compute elements corresponding to those in $\text{vech}(T)$ that are not fixed by sparsity. For instance, to compute the second term in $\nabla_{\text{vech}(T)} F(\lambda)$, we just find $u = T^{-\top}z$ and $v = T^{-1}\nabla_\theta^2 h(\theta) g(\lambda, \theta)$, and then form $u_i v_j$ for nonzero elements (i, j) of T.

The update for T in SGD does not ensure positiveness of the diagonal entries. Hence, we introduce T^* such that $T_{ii}^* = \log(T_{ii})$ for $i = 1, \ldots, n$, and $T_{ij}^* = T_{ij}$ *for* $i \neq j$. Let J be a $d \times d$ matrix with diagonal equal to $\text{diag}(T)$ and all off-diagonal entries being 1, and D be a diagonal matrix with the diagonal given by $\text{vech}(J)$. Then $\nabla_{\text{vech}(T^*)} F(\lambda) = D\nabla_{\text{vech}(T)} F(\lambda)$ and updates for T^* are unconstrained.

Table 4 outlines the SGD algorithms for updating (μ, T) by minimizing the Fisher, score-based or KL (derived in Tan and Nott, 2018) divergences. The stepsize ρ_t is computed elementwise adaptively using Adadelta

KLD	FDr and SDr

Initialize μ and T. For $t = 1, 2, \ldots N$,
   1. Generate $z \sim N(0, I_d)$.
   2. Compute $u = T^{-\top}z$, $\theta = \mu + u$ and $g = \nabla_\theta \log h(\theta) + Tz$.	

3. $\mu \leftarrow \mu + \rho_t g$.
 4. $v = T^{-1}g$.
 5. $g_T = -uv^\top$.
 6. $T^* \leftarrow T^* + \rho_t \, Dg_T$.
 7. Obtain T from T^*.
	3. If SD,
	   • $g \leftarrow T^{-1}g$.
	   • $z \leftarrow z - g$
	   • $g \leftarrow T^{-\top}g$.
	 4. $w = \nabla_\theta^2 \log h(\theta)g$,
	    $v = T^{-1}w$.
	 5. $\mu \leftarrow \mu - 2\rho_t w$.
	 6. $g_T = gz^\top - uv^\top$.
	 7. $T^* \leftarrow T^* - 2\rho_t Dg_T$.
	 8. Obtain T from T^*.

TABLE 4

SGD algorithms based on reparametrization trick.

(Zeiler, 2012). All three algorithms compute $g(\lambda, \theta)$, but the KLD based algorithm uses $g(\lambda, \theta)$ directly to update μ and T, while the FD and SD based algorithms use the Hessian $\nabla_\theta^2 \log h(\theta)$ to condition $g(\lambda, \theta)$ and are hence more computationally intensive.

5.1 Analysis of variance of gradient estimates

We study variance of the unbiased gradient estimates derived by applying the reparametrization trick on the KL, Fisher and score-based divergences, to examine effects of the conditioning matrix, $\nabla_\theta^2 \log h(\theta)$. The variance of these gradients plays a crucial role in the stability of the optimization, as large variance can cause a zigzag phenomenon, making convergence difficult. For a closed form analysis, we assume the target $p(\theta|y)$ is $N(\nu, \Lambda^{-1})$. Then $\nabla_\theta \log h(\theta) = -\Lambda(\theta - \nu)$ and $\nabla_\theta^2 \log h(\theta) = -\Lambda$.

From Table 4, gradient estimates with respect to μ for the KL, Fisher and score-based divergences based on a single sample are

$$g_\mu^{\text{KL}} = Az - \Lambda(\mu - \nu), \quad g_\mu^{\text{F}} = 2\Lambda g_\mu^{\text{KL}}, \quad g_\mu^{\text{S}} = 2\Lambda\Sigma g_\mu^{\text{KL}},$$

where $A = T - \Lambda T^{-\top}$. The stochasticity stems from drawing $z \sim N(0, I_d)$ and $\text{Var}(g_\mu^{\text{KL}}) = AA^\top$, while

$$\text{Var}(g_\mu^{\text{F}}) = 4\Lambda\text{Var}(g_\mu^{\text{KL}})\Lambda, \quad \text{Var}(g_\mu^{\text{S}}) = 4\Lambda\Sigma\text{Var}(g_\mu^{\text{KL}})\Sigma\Lambda.$$

Similarly, from Table 4, the gradient estimates with respect to T are

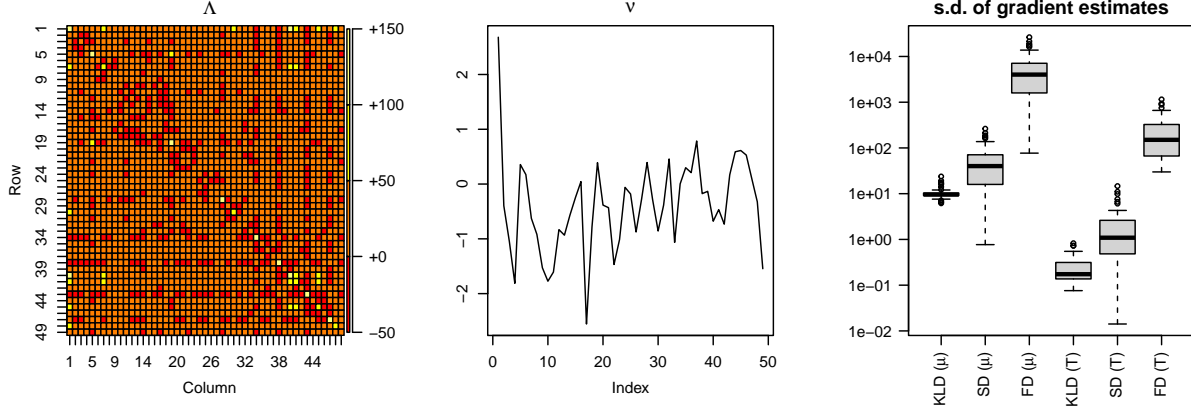$$g_T^{\text{KL}} = T^{-\top}z(\mu - \nu)^\top \Lambda T^{-\top} - T^{-\top}zz^\top A^\top T^{-\top},$$

10

Fig 4: First two plots show the true precision matrix Λ and mean ν, and the third plot contains boxplots of the standard deviation (s.d.) in gradient estimates for $\{\mu_i\}$ and $\{T_{ii}\}$.

$$g_T^{\mathrm{F}} = 2\{\Lambda(\mu-\nu)z^\top + T^{-\top}z(\mu-\nu)^\top\Lambda^2 T^{-\top}$$
$$- Azz^\top - T^{-\top}zz^\top A^\top \Lambda T^{-\top}\},$$

$$g_T^{\mathrm{S}} = 2[\Sigma\Lambda(\mu-\nu)\{z^\top T^{-1} + (\mu-\nu)^\top\}\Lambda T^{-\top}$$
$$- \Sigma A\{zz^\top T^{-1} + z(\mu-\nu)^\top\}\Lambda T^{-\top}$$
$$+ T^{-\top}\{z(\mu-\nu)^\top\Lambda - zz^\top A^\top\}\Sigma\Lambda T^{-\top}].$$

The variance of these gradient estimates depends on the mean and precision of the true target, which is fixed, and that of the variational approximation, which keeps changing during SGD. Suppose Λ and T are both diagonal matrices, then

$$\mathrm{Var}(g_{\mu_i}^{\mathrm{KL}}) = T_{ii}^2 - 2\Lambda_{ii} + \Lambda_{ii}^2 T_{ii}^{-2},$$

$$\mathrm{Var}(g_{\mu_i}^{\mathrm{F}}) = 4\Lambda_{ii}^2\mathrm{Var}(g_{\mu_i}^{\mathrm{KL}}),$$

$$\mathrm{Var}(g_{\mu_i}^{\mathrm{S}}) = (4\Lambda_{ii}^2/T_{ii}^4)\,\mathrm{Var}(g_{\mu_i}^{\mathrm{KL}}),$$

$$\mathrm{Var}(g_{T_{ii}}^{\mathrm{KL}}) = T_{ii}^{-4}\left\{\Lambda_{ii}^2(\mu_i-\nu_i)^2 + 2\left(T_{ii} - \Lambda_{ii}/T_{ii}\right)^2\right\},$$

$$\mathrm{Var}(g_{T_{ii}}^{\mathrm{F}}) = 4(T_{ii}^2 + \Lambda_{ii})^2\mathrm{Var}(g_{T_{ii}}^{\mathrm{KL}}).$$

$$\mathrm{Var}(g_{T_{ii}}^{\mathrm{S}}) = 4\Lambda_{ii}^2 T_{ii}^{-8}\left\{\left(3\Lambda_{ii} - T_{ii}^2\right)^2(\mu_i-\nu_i)^2\right.$$
$$\left. + 8\left(T_{ii} - \Lambda_{ii}/T_{ii}\right)^2\right\}.$$

It can be verified that these variances are zero at full convergence, when $\mu_i = \nu_i$ and $T_{ii}^2 = \Lambda_{ii} \,\forall\, i$. The variance of gradients with respect to μ of FD and SD are larger than that of KLD if $\Lambda_{ii} > 0.5$ and $\Lambda_{ii}/T_{ii}^2 > 0.5$ respectively. Assuming $\mu_i = \nu_i$ for the SD, the variance of gradients with respect to T of FD and SD are larger than that of KLD if $T_{ii}^2 + \Lambda_{ii} > 0.5$ and $\Lambda_{ii}/T_{ii}^2 > 0.25$ respectively.

In summary, the variance of gradient estimates based on FD is larger than that of KL once $\Lambda_{ii} > 0.5$ regardless of the values of the variational parameters, and variance inflation is larger for T than μ. For SD, the inflation factor involves the ratio Λ_{ii}/T_{ii}^2, so variance inflation relative to KLD can be reduced if $T_{ii}^2 > \Lambda_{ii}$.

Next, we investigate the variance of gradient estimates for a multivariate Gaussian target with $d = 49$ in a real setting. The true precision matrix Λ and mean ν, visualized in the first two plots of Fig 4, are derived from MCMC samples obtained by fitting a logistic regression model to the German credit data in Section 7.1. The diagonal entries of Λ range from 0.52 to 148.82 with a mean of 45.68. We set $T = 10I_d$ and $\mu = 0$ to represent an uninformative initialization. The stochastic gradients with respect to μ and T are computed for each divergence by generating $z \sim \mathrm{N}(0, I_d)$ for 1000 iterations. The standard deviation of these gradient estimates are calculated for μ_i and T_{ii} for $i = 1, \ldots, d$, and summarized using boxplots in Fig 4. The y-axis of the boxplots has a log scale. KLD has the smallest standard deviation, followed by SD, while the standard deviation of FD is much larger than SD and KLD for both μ and T. Although Λ is not a diagonal matrix, these findings are consistent with our earlier analysis. This example highlights the difficulty in using SGD to minimize the FD and SD due to the much larger variance in gradient estimates relative to KLD, which motivates an alternative optimization procedure described next.

11

6. SGD BASED ON BATCH APPROXIMATION

Unbiased gradient estimates based on the reparametrization trick involve the Hessian $\nabla_\theta^2 \log h(\theta)$, which is computationally expensive, requires high storage and increases the variability in gradient estimates. This can lead to instability in minimizing the FD and SD. To address these challenges, we propose an alternative approach that eliminates dependence on the Hessian, by minimizing biased estimates of the FD and SD computed using a batch of samples randomly selected from the current variational approximation at each iteration. First, the SD and FD can be written respectively as

$$S_{q_\lambda}(\lambda) = \mathrm{E}_{q_\lambda} \|g_h(\theta) + \Sigma^{-1}(\theta - \mu)\|_\Sigma^2$$

$$= \mathrm{E}_{q_\lambda} \Big\{ g_h(\theta)^\top \Sigma g_h(\theta) + 2g_h(\theta)^\top(\theta - \mu)$$

$$+ (\theta - \mu)^\top \Sigma^{-1}(\theta - \mu) \Big\},$$

$$F_{q_\lambda}(\lambda) = \mathrm{E}_{q_\lambda} \|g_h(\theta) + \Sigma^{-1}(\theta - \mu)\|^2$$

$$= \mathrm{E}_{q_\lambda} \Big\{ g_h(\theta)^\top g_h(\theta) + 2g_h(\theta)^\top \Sigma^{-1}(\theta - \mu)$$

$$+ (\theta - \mu)^\top \Sigma^{-2}(\theta - \mu) \Big\},$$

where $g_h(\theta) = \nabla_\theta \log h(\theta)$ and the subscript q_λ emphasizes that expectation is with respect to $q_\lambda(\theta)$. To estimate SD and FD at the t-iteration, we generate B samples $\{\theta_1, \ldots, \theta_B\}$ from the current estimate of the variational density $q_t(\theta) = \mathrm{N}(\theta|\mu^{(t)}, \Sigma^{(t)})$. This can be done by generating $z_i \sim \mathrm{N}(0, I_d)$ and computing $\theta_i = \mu^{(t)} + T^{(t)-\top}z_i$ for $i = 1, \ldots, B$, where $\Sigma^{(t)} = T^{(t)-\top}T^{(t)-1}$. Let

$$\bar{\theta} = \frac{1}{B}\sum_{i=1}^B \theta_i, \quad \bar{g}_h = \frac{1}{B}\sum_{i=1}^B g_h(\theta_i),$$

$$C_{\theta g} = \frac{1}{B}\sum_{i=1}^B (\theta_i - \bar{\theta})(g_h(\theta_i) - \bar{g}_h)^\top,$$

(8)

$$C_\theta = \frac{1}{B}\sum_{i=1}^B (\theta_i - \bar{\theta})(\theta_i - \bar{\theta})^\top,$$

$$C_g = \frac{1}{B}\sum_{i=1}^B (g_h(\theta_i) - \bar{g}_h)(g_h(\theta_i) - \bar{g}_h)^\top,$$

be summary statistics based on the batch of samples. Estimates of SD and FD are

$$\hat{S}_{q_t}(\lambda) = \frac{1}{B}\sum_{i=1}^B \Big\{ g_h(\theta_i)^\top \Sigma g_h(\theta_i) + 2g_h(\theta_i)^\top(\theta_i - \mu)$$

$$+ (\theta_i - \mu)^\top \Sigma^{-1}(\theta_i - \mu) \Big\}$$

$$= \mathrm{tr}(V\Sigma) + \mathrm{tr}(U\Sigma^{-1}) + 2\mathrm{tr}(W),$$

$$\hat{F}_{q_t}(\lambda) = \frac{1}{B}\sum_{i=1}^B \Big\{ g_h(\theta_i)^\top g_h(\theta_i) + 2g_h(\theta_i)^\top \Sigma^{-1}(\theta_i - \mu)$$

$$+ (\theta_i - \mu)^\top \Sigma^{-2}(\theta_i - \mu) \Big\}$$

$$= \mathrm{tr}(V) + \mathrm{tr}(U\Sigma^{-2}) + 2\mathrm{tr}(W\Sigma^{-1}),$$

where $U = C_\theta + (\mu - \bar{\theta})(\mu - \bar{\theta})^\top$, $V = C_g + \bar{g}_h\bar{g}_h^\top$ and $W = C_{\theta g} - (\mu - \bar{\theta})\bar{g}_h^\top$. Differentiating with respect to μ and T,

(9)
$$\nabla_\mu \hat{S}_{q_t}(\lambda) = 2\Sigma^{-1}(\mu - \bar{\theta}) - 2\bar{g}_h,$$

$$\nabla_\mu \hat{F}_{q_t}(\lambda) = \Sigma^{-1}\nabla_\mu \hat{S}_{q_t}(\lambda),$$

$$\nabla_{\mathrm{vech}(T)} \hat{S}_{q_t}(\lambda) = 2\mathrm{vech}(UT - \Sigma V T^{-\top}),$$

$$\nabla_{\mathrm{vech}(T)} \hat{F}_{q_t}(\lambda) = 2\mathrm{vech}\{(W + W^\top + \Sigma^{-1}U$$

$$+ U\Sigma^{-1})T\}.$$

These gradient estimates of SD and FD are biased because the θ's are replaced by samples $\{\theta_1, \ldots, \theta_B\}$ generated from $q_t(\theta) = \mathrm{N}(\theta|\mu^{(t)}, \Sigma^{(t)})$, and are no longer functions of (μ, Σ) when we derive the gradients. The dependence on λ through θ has been cut. On the other hand, the reparametrization trick in Section 5 produces unbiased estimates because the θ's are regarded as samples from $q(\theta) = \mathrm{N}(\theta|\mu, \Sigma)$, and remain functions of (μ, Σ) when the chain rule is applied to find the gradients.

With the batch approximation, all gradients are independent of the Hessian, which reduces computation costs significantly and enhances stability during optimization. As before, we only update elements of $\mathrm{vech}(T)$ not fixed by sparsity, and ensure positivity of diagonal entries in T by applying a transformation. SGD algorithms for updating (μ, T) based on minimizing the batch approximated FD and SD are outlined in Table 5.

FDb	SDb
Initialize μ and T. For $t = 1, \ldots N$,	
1. Generate $z_i \sim \mathrm{N}(0, I_d)$ and compute $\theta_i = \mu + T^{-\top} z_i$ for $i = 1, \ldots B$.	
2. Compute $g_h(\theta_i)$ for $i = 1, \ldots B$ and the summary statistics in (8).	
3. $U = C_\theta + (\mu - \overline{\theta})(\mu - \overline{\theta})^\top$.	
4. $g\mu = 2TT^\top(\mu - \overline{\theta}) - 2\overline{g}_h$.	
5. $\mu \leftarrow \mu - \rho_t TT^\top g\mu$	5. $\mu \leftarrow \mu - \rho_t g\mu$.
6. $W = C_{\theta g} - (\mu - \overline{\theta})\overline{g}_h^\top$.	6. $V = C_g + \overline{g}_h\overline{g}_h^\top$.
7. $g_T = 2(W + W^\top + TT^\top U + UTT^\top)T$.	7. $g_T = 2(UT - T^{-\top}T^{-1}VT^{-\top})$.
8. $T^* \leftarrow T^* - \rho_t Dg_T$.	
9. Obtain T from T^*.	

<div align="center">TABLE 5</div>

SGD algorithms based on batch approximated FD and SD.

6.1 Interpretation and related methods

Previously, Elkhalil et al. (2021) have designed autoencoders based on minimizing a batch approximation of the Fisher divergence using SGD. Cai et al. (2024) also proposed a BaM algorithm that derived closed form updates of (μ, Σ) by minimizing the objective,

$$\hat{S}_{q_t}(\lambda) + (2/\rho_t)\mathrm{KL}(q_t \| q_\lambda),$$

with respect to λ at the tth iteration, where $\rho_t = Bd/t$ is the learning rate. BaM can be interpreted as a proximal point method that produces a sequence of variational densities $q_0, q_1, \ldots$ such that q_{t+1} matches the scores $g_h(\theta)$ at $\{\theta_1, \ldots, \theta_B\}$ on average better than q_t, while the KLD based penalty term ensures stability by preventing q_{t+1} from deviating too much from q_t. Similarly, the SGD algorithm in Table 5 can be interpreted as minimizing

$$\hat{S}_{q_t}(\lambda) + (1/2\rho_t)\|\lambda - \lambda_t\|^2$$

with respect to λ, where an ℓ_2 penalty is used instead, and a linear approximation of $\hat{S}_{q_t}(\lambda)$ at λ_t is considered. Then

$$\lambda_{t+1} = \arg\min_\lambda \left\{ \hat{S}_{q_t}(\lambda_t) + \nabla_\lambda \hat{S}_{q_t}(\lambda_t)^\top(\lambda - \lambda_t) \right.$$
$$\left. + (1/2\rho_t)\|\lambda - \lambda_t\|^2 \right\} = \lambda_t - \rho_t \nabla_\lambda \hat{S}_{q_t}(\lambda_t),$$

which corresponds to the SGD update with step size ρ_t employed in Table 5. This discussion extends similarly to the Fisher divergence.

Instead of viewing (9) as biased estimates of the gradients of SD and FD, we can consider $\hat{S}_{q_t}(\lambda)$ and $\hat{F}_{q_t}(\lambda)$ as new objectives, which measure the divergence between $q_\lambda(\theta)$ and $p(\theta|y)$ based on their gradients evaluated at randomly selected samples at each iteration. Indeed, $\hat{S}_{q_t}(\lambda)$ and $\hat{F}_{q_t}(\lambda)$ reduce to zero when $q_\lambda(\theta) = p(\theta|y)$. At each iteration t, q_{t+1} updates q_t so as to reduce the difference in gradients between q_t and the true posterior when evaluated on the randomly selected batch of samples. As q_t converges to $p(\theta|y)$, the samples also shift towards the region where the true posterior has high probability mass. Figure 5 illustrates the progression of SDb with batch size $B = 5$ using $\mathrm{N}(2, 1.5)$ as target. As optimization proceeds, SDb gradually refines the variational density by emulating the gradients of the target on the batch of samples and converges steadily toward the target.

The SGD algorithm in Table 5 differs from BaM in several key aspects. While BaM relies on KLD regularization to stabilize updates and has closed-form updates for (μ, Σ), we use an ℓ_2 penalty and a linearization of the batch approximation leading to SGD. By avoiding linearization of $\hat{S}_{q_t}(\lambda)$ and SGD, the number of iterations required for convergence is reduced in BaM, but each BaM iteration is expensive as the closed form update of Σ involves inverting a $d \times d$ matrix with cost of $\mathcal{O}(d^3)$, although this can be reduced to $\mathcal{O}(d^2 B + B^3)$ for small batch size B through low rank solvers. This high cost can result in long runtimes in high dimensions. Moreover, BaM is designed for full covariance matrices and it is not clear how sparsity can be enforced in the precision matrix
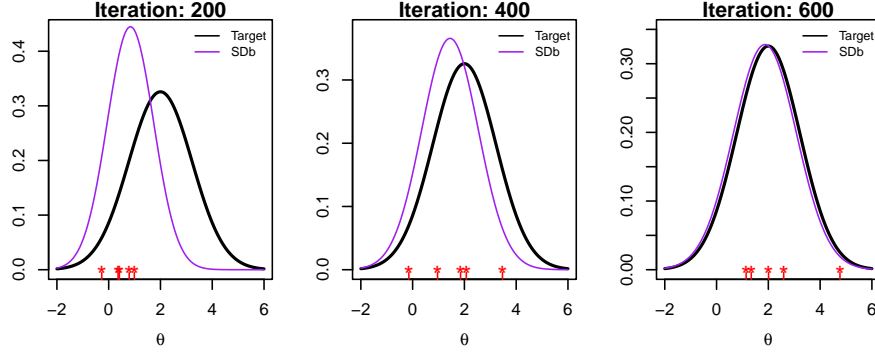
Fig 5: Progression of SDb for a Gaussian target where the red $*$'s mark the randomly chosen samples.

to take advantage of the posterior conditional independence structure in hierarchical models. BaM can also run into instability and numerical issues with ill-conditioned matrices in practice, which may not be alleviated even with larger batch sizes. On the other hand, SGD allows updating of the Cholesky factor of the precision matrix, where sparse structures can be easily enforced. Smaller batches can also be used, which further reduces the computation and storage burden. While BaM is suited for full covariance Gaussian VI, our approach provides a more scalable and stable alternative for high-dimensional hierarchical models with conditional independence structure.

6.2 Batch approximated objective under mean-field

Next, we investigate behavior of the batch approximated FD and SD under the mean-field assumption considered in Section 2. Suppose the target $p(\theta|y)$ is $N(\nu, \Lambda^{-1})$ with non-diagonal precision matrix Λ, and the variational approximation $q(\theta)$ is $N(\mu, \Sigma)$ where Σ is a diagonal matrix. Using $B > 1$ samples $\{\theta_1, \ldots, \theta_B\}$ from an estimate of q, $\hat{q}(\theta) = N(\hat{\mu}, \hat{\Sigma})$, where $\hat{\Sigma}$ is also a diagonal matrix, the batch approximated SD and FD are

$$\hat{S}_q(\lambda) = \sum_{i=1}^{d} (V_{ii}\Sigma_{ii} + U_{ii}\Sigma_{ii}^{-1}) + 2\text{tr}(W),$$

$$\hat{F}_q(\lambda) = \sum_{i=1}^{d} (U_{ii}\Sigma_{ii}^{-2} + 2W_{ii}\Sigma_{ii}^{-1}) + \text{tr}(V).$$

LEMMA 2. $\hat{S}_q(\lambda)$ is minimized at $\Sigma_{ii}^{\hat{S}} = \sqrt{C_{\theta,ii}/C_{g,ii}}$ and $\mu_i^{\hat{S}} = \bar{\theta}_i + \bar{g}_{h,i}\Sigma_{ii}^{\hat{S}}$ for $i = 1, \ldots, d$. If the diagonal entries of $C_{\theta g}$ are all negative, then $\hat{F}_q(\lambda)$ is mini-

mized at $\Sigma_{ii}^{\hat{F}} = -C_{\theta,ii}/C_{\theta g,ii}$ and $\mu_i^{\hat{F}} = \bar{\theta}_i + \bar{g}_{h,i}\Sigma_{ii}^{\hat{F}}$ for $i = 1, \ldots, d$.

PROOF. Differentiating $\hat{S}_q(\lambda)$ and $\hat{F}_q(\lambda)$ with respect to μ and Σ_{ii}, we obtain

$$\nabla_\mu \hat{S}_q(\lambda) = 2\Sigma^{-1}(\mu - \bar{\theta}) - 2\bar{g}_h,$$

$$\nabla_\mu \hat{F}_q(\lambda) = \Sigma^{-1}\nabla_\mu \hat{S}_q(\lambda),$$

$$\nabla_{\Sigma_{ii}} \hat{S}_q(\lambda) = V_{ii} - U_{ii}\Sigma_{ii}^{-2},$$

$$\nabla_{\Sigma_{ii}} \hat{F}_q(\lambda) = -2\Sigma_{ii}^{-2}(U_{ii}\Sigma_{ii}^{-1} + W_{ii}).$$

Setting these derivatives to zero yields
(10)

$$\mu_i^{\hat{S}} = \bar{\theta}_i + \Sigma_{ii}^{\hat{S}}\bar{g}_{h,i}, \quad V_{ii}(\Sigma_{ii}^{\hat{S}})^2 = C_{\theta,ii} + (\mu_i^{\hat{S}} - \bar{\theta}_i)^2,$$

$$\mu_i^{\hat{F}} = \bar{\theta}_i + \Sigma_{ii}^{\hat{F}}\bar{g}_{h,i}, \quad \Sigma_{ii}^{\hat{F}} = -\frac{C_{\theta,ii} + (\mu_i^{\hat{F}} - \bar{\theta}_i)^2}{C_{\theta g,ii} - \bar{g}_{h,i}(\mu_i^{\hat{F}} - \bar{\theta}_i)}.$$

Solving these equations simultaneously, we obtain

$$V_{ii}(\Sigma_{ii}^{\hat{S}})^2 = C_{\theta,ii} + (\Sigma_{ii}^{\hat{S}})^2\bar{g}_{h,i}^2 \implies \Sigma_{ii}^{\hat{S}} = \sqrt{C_{\theta,ii}/C_{g,ii}},$$

$$\Sigma_{ii}^{\hat{F}} = -\{C_{\theta,ii} + (\Sigma_{ii}^{\hat{F}})^2\bar{g}_{h,i}^2\}/\{C_{\theta g,ii} - \Sigma_{ii}^{\hat{F}}\bar{g}_{h,i}^2\}$$

$$\implies \Sigma_{ii}^{\hat{F}} = -C_{\theta,ii}/C_{\theta g,ii}.$$

Plugging these values into (10) yields corresponding values for $\mu_i^{\hat{S}}$ and $\mu_i^{\hat{F}}$. ☐

Next, we study limiting behavior of the batch approximated SD and FD as the batch size $B \to \infty$. Theorem 2 relies on the limits of summary statistics in (8) presented in Lemma 3.

LEMMA 3. Suppose $\{\theta_1, \ldots, \theta_B\}$ are samples from $\hat{q}(\theta) = N(\hat{\mu}, \hat{\Sigma})$ and the target is $p(\theta|y) = N(\nu, \Lambda^{-1})$. As

14

$B \to \infty$, *the summary statistics in* (8) *satisfy*

$$\overline{\theta} \xrightarrow{a.s.} \hat{\mu}, \quad C_\theta \xrightarrow{a.s.} \hat{\Sigma}, \quad \overline{g}_h \xrightarrow{a.s.} \Lambda(\nu - \hat{\mu}),$$

$$C_g \xrightarrow{a.s.} \Lambda\hat{\Sigma}\Lambda, \quad C_{\theta g} \xrightarrow{a.s.} -\hat{\Sigma}\Lambda.$$

PROOF. The first two results follow directly from the law of large numbers. For the target, $g_h(\theta_i) = -\Lambda(\theta_i - \nu)$. Thus $\overline{g}_h = -\Lambda(\overline{\theta} - \nu)$ and $g_h(\theta_i) - \overline{g}_h = -\Lambda(\theta_i - \overline{\theta})$.

$$\therefore \quad C_g = \frac{1}{B}\sum_{i=1}^{B}\Lambda(\theta_i - \overline{\theta})(\theta_i - \overline{\theta})^\top\Lambda = \Lambda C_\theta \Lambda,$$

$$C_{\theta g} = -\frac{1}{B}\sum_{i=1}^{B}(\theta_i - \overline{\theta})(\theta_i - \overline{\theta})^\top\Lambda = -C_\theta\Lambda.$$

By the continuous mapping theorem (Durrett, 2019), $\overline{g}_h \xrightarrow{a.s.} \Lambda(\nu - \hat{\mu})$, $C_g \xrightarrow{a.s.} \Lambda\hat{\Sigma}\Lambda$ and $C_{\theta g} \xrightarrow{a.s.} -\hat{\Sigma}\Lambda$. $\square$

THEOREM 2. *Suppose the target* $p(\theta|y)$ *is* $N(\nu, \Lambda^{-1})$. *Let the variational approximation* $q(\theta)$ *be* $N(\mu, \Sigma)$, *and* $\hat{q}(\theta) = N(\theta|\hat{\mu}, \hat{\Sigma})$ *be an estimate of* $q(\theta)$, *where* Σ *and* $\hat{\Sigma}$ *are both diagonal matrices. As the batch size* $B \to \infty$, *the batch approximated SD and FD are minimized at* $(\mu^{\hat{S}}, \Sigma^{\hat{S}})$ *and* $(\mu^{\hat{F}}, \Sigma^{\hat{F}})$ *respectively, where*

$$\Sigma_{ii}^{\hat{S}} \xrightarrow{a.s.} \sqrt{\frac{\hat{\Sigma}_{ii}}{\sum_{j=1}^{d}\hat{\Sigma}_{jj}\Lambda_{ij}^2}}, \qquad \Sigma_{ii}^{\hat{F}} \xrightarrow{a.s.} \frac{1}{\Lambda_{ii}},$$

$$\mu_i^{\hat{S}} \xrightarrow{a.s.} \hat{\mu}_i + \sqrt{\frac{\hat{\Sigma}_{ii}}{\sum_{j=1}^{d}\hat{\Sigma}_{jj}\Lambda_{ij}^2}}\sum_{j=1}^{d}\Lambda_{ij}(\nu_j - \hat{\mu}_j),$$

$$\mu_i^{\hat{F}} \xrightarrow{a.s.} \hat{\mu}_i + \frac{1}{\Lambda_{ii}}\sum_{j=1}^{d}\Lambda_{ij}(\nu_j - \hat{\mu}_j).$$

PROOF. Results can be obtained by applying the continuous mapping theorem on Lemma 2 and using the results in Lemma 3. Note that $(\Lambda\hat{\Sigma}\Lambda)_{ii} = \sum_{j=1}^{d}\hat{\Sigma}_{jj}\Lambda_{ij}^2$ and $(\hat{\Sigma}\Lambda)_{ii} = \hat{\Sigma}_{ii}\Lambda_{ii}$. $\square$

From Lemma 3, $C_{\theta g}$ converges almost surely to $-\hat{\Sigma}\Lambda$, with ith diagonal entry $-\hat{\Sigma}_{ii}\Lambda_{ii} < 0$. Thus, diagonal elements of $C_{\theta g}$ are likely negative for a sufficiently large B, but may be positive for a small batch size B. In that case, assuming $\mu_i = \overline{\theta}_i + \Sigma_{ii}\overline{g}_{h,i}$, $\nabla_{\Sigma_{ii}}\hat{F}_q(\lambda) = -2\Sigma_{ii}^{-2}(C_{\theta,ii} + C_{\theta g,ii}) < 0$, and $\hat{F}_q(\lambda)$ decreases monotonically as $\Sigma_{ii} \to \infty$. Thus the batch approximated FD faces the issue of "variance explosion". This is in stark

contrast to results in Section 2 where the FD has a closed form solution. On the other hand, the batch approximated SD no longer faces the issue of "variational collapse", and has a closed form solution for any $B > 1$. As $B \to \infty$, $\Sigma_{ii}^{\hat{S}} \xrightarrow{a.s.} \sqrt{\hat{\Sigma}_{ii}/(\sum_{j=1}^{d}\hat{\Sigma}_{jj}\Lambda_{ij}^2)}$, the limit of which is equal to that in (1) where $M = \hat{\Sigma}$ in the weighted Fisher divergence. It follows from Theorem 1 that $\Sigma_{ii}^{\hat{S}} \leq \Sigma_{ii}^{\hat{F}} = \Sigma_{ii}^{\text{KL}}$ in the limit of infinite batch size. Thus the batch approximated SD underestimates the posterior variance more severely than the batch approximated FD, for which the posterior variance estimate matches that of the KLD, as $B \to \infty$. However, unlike the FD and SD, the true mean ν is not recovered by the batch approximated FD and SD even as $B \to \infty$, unless Λ is a diagonal matrix.

7. APPLICATIONS

We evaluate the performance of algorithms in Tables 4 and 5 by applying them to logistic regression, GLMMs and stochastic volatility models, and compare their results with BaM and MCMC. MCMC sampling is performed using RStan by running two chains in parallel, each with 50,000 iterations. The first half is discarded as burn-in, while the remaining 50,000 draws are used to compute kernel density estimates, regarded as the gold standard.

To evaluate the multivariate accuracy of variational approximation relative to MCMC, we use maximum mean discrepancy (MMD, Zhou et al., 2023). We calculate $M^* = -\log(\text{MMD}_u^2 + 10^{-5})$, where

$$\text{MMD}_u^2 = \frac{1}{m(m-1)}\sum_{i \neq j}^{m}[k(\mathbf{x}_v^{(i)}, \mathbf{x}_v^{(j)}) + k(\mathbf{x}_g^{(i)}, \mathbf{x}_g^{(j)})$$

$$- k(\mathbf{x}_v^{(i)}, \mathbf{x}_g^{(j)}) - k(\mathbf{x}_v^{(j)}, \mathbf{x}_g^{(i)})],$$

$\mathbf{x}_v^{(1)}, \ldots, \mathbf{x}_v^{(m)}$ and $\mathbf{x}_g^{(1)}, \ldots, \mathbf{x}_g^{(m)}$ represent independent samples drawn from the variational approximation and MCMC respectively, k is the radial basis kernel function and $m = 1000$. M^* is computed 50 times for each variational approximation and a higher value indicates better multivariate accuracy. In addition, we assess the ability to capture the marginal mode of each variable accurately using the normalized absolute difference in mode ($|\mu - \mu^*|/\sigma^*$), where μ^* and σ^* denote the mode and standard deviation of each variable based on MCMC samples.

To assess convergence, we track unbiased estimates of the lower bound, $\hat{\mathcal{L}}$, averaged over every 1000 iterations for SGD methods and 50 iterations for BaM, to reduce noise. Less iterations are used for averaging in BaM, as it uses closed form updates, which leads to more stable trajectories with reduced oscillations. Moreover, BaM usually requires a larger batch size and converges faster than SGD methods. Each algorithm is terminated when the gradient of a linear regression line fitted to the past five lower bound averages is less than 0.01, or when the maximum number of iterations is reached. The batch size of FDb and SDb is adjusted according to model complexity, and larger batch sizes are used for more complex models. All experiments are performed on a 16GB Apple M1 computer, using R and Julia 1.11.2.

7.1 Logistic regression

Consider a logistic regression model where $y = (y_1, \ldots, y_n)^\top$ represents n independent binary responses. Each y_i follows a Bernoulli distribution with success probability p_i, modeled as

$$\text{logit}(p_i) = X_i^\top \theta \quad \text{for} \quad i = 1, \ldots, n,$$

where $X_i \in \mathbb{R}^d$ denotes the covariates of the ith observation and $\theta \in \mathbb{R}^d$ denotes the unknown coefficients, which is assigned the prior $\mathrm{N}(0, \sigma_0^2 I_d)$ with $\sigma_0^2 = 100$. Here, the precision matrix of the Gaussian variational approximation is not sparse, but a full matrix. The log joint density of the model, gradient and Hessian are given by

$$\log h(\theta) = y^\top X\theta - \sum_{i=1}^n \log\{1 + \exp(X_i^\top \theta)\}$$
$$- \tfrac{d}{2}\log(2\pi\sigma_0^2) - \theta^\top\theta/(2\sigma_0^2),$$
$$\nabla_\theta \log h(\theta) = X^\top(y - w) - \theta/\sigma_0^2,$$
$$\nabla_\theta^2 \log h(\theta) = -X^\top W X - I_d/\sigma_0^2,$$

where $w = (w_1, \ldots, w_n)^\top$, $w_i = \{1 + \exp(-X_i^\top\theta)\}^{-1}$ for $i = 1, \ldots, n$, W is an $n \times n$ diagonal matrix with diagonal entries $w_i(1 - w_i)$ and $X = (X_1, \ldots, X_n)^\top$.

We fit the logistic regression model to two real datasets from the UCI machine learning repository. The first is the German credit data, which consists of 1000 individuals classified as having a "good" or "bad" credit risk,

and 20 attributes. All quantitative predictors are standardized to have mean zero and standard deviation one, while qualitative predictors are encoded using dummy variables. The second is the Adult data with $48,842$ observations, which is used to predict whether an individual's annual income exceeds $\$50,000$ based on 14 attributes. For MCMC to be feasible, we use the preprocessed a4a data at www.csie.ntu.edu.tw/~cjlin/libsvmtools/datasets/binary.html, which has 4781 training samples derived from the Adult data. After preprocessing, $d = 49$ for German credit data and $d = 124$ for a4a data. As the a4a data is high dimensional and has a large number of observations, we only generate $10,000$ MCMC samples from two parallel chains, each consisting of $10,000$ iterations. We use a batch size of $B = 3$ for FDb and SDb, and $B = 50$ for BaM. The maximum number of iterations is $60,000$.
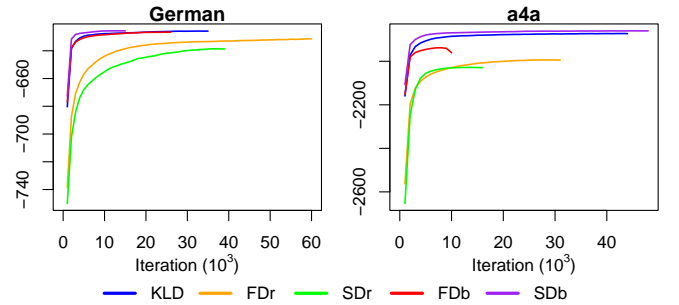

Fig 6: German credit and a4a data. Average lower bound over every 1000 iterations.

Fig 6 shows progression of the lower bound for SGD methods. FDr and SDr converge very slowly, and attain much poorer lower bounds than other methods at termination. This is likely due to the high variance in their gradient estimates, as discussed in Section 5.1. In contrast, SDb converges rapidly and achieves the highest lower bound within the first one thousand iterations, surpassing even KLD. The lower bound achieved by FDb, on the other hand, is lower than KLD and SDb although it performs better than FDr and SDr.

From the MMD results in Table 6, FDr and SDr produce much poorer variational approximations than KLD, while FDb and SDb provide significant improvements over FDr and SDr. In particular, SDb produced results

		KLD	FDr	SDr	FDb	SDb	BaM	MCMC
MMD	German	8.82±1.72	1.11±0.02	0.75±0.01	2.86±0.07	8.37±1.28	8.29±1.35	-
	a4a	2.49±0.03	0.71±0.02	0.71±0.01	1.61±0.02	3.04±0.04	5.22±0.08	-
$\frac{|\mu - \mu^*|}{\sigma^*}$	German	0.08±0.05	0.55±0.68	0.74±0.62	0.25±0.27	0.08±0.06	0.08±0.05	-
	a4a	0.18±0.15	0.45±0.52	0.38±0.43	0.40±0.43	0.15±0.15	0.14±0.16	-
time	German	3.2 (35)	15.0 (60)	9.8 (39)	6.2 (26)	3.8 (15)	1.6 (0.35)	354.4
	a4a	19.2 (44)	108.5 (31)	55.2 (16)	14.0 (10)	70.4 (48)	13.6 (1.05)	28556.1

TABLE 6

Logistic regression. Estimates of mean and standard deviation for MMD and normalized absolute difference in mode. Runtime is in seconds and number of iterations (in thousands) is given in brackets.

comparable to KLD for the German credit data, and better than KLD for the a4a data. In terms of runtime, KLD is the fastest among SGD methods. For the German credit data, FDr, SDr, FDb and SDb each takes $\sim$0.25s per 1000 iterations, but FDb and SDb require less iterations to converge. For the a4a data, FDr and SDr require $\sim$3.5s per 1000 iterations compared to $\sim$1.5s for FDb and SDb, due to the larger cost of computing the Hessian in high dimensions. BaM converges most rapidly, outperforming all SGD methods in runtime. Its MMD values are comparable to KLD for the German credit data, and much higher than SGD methods for the a4a data.

Overall, MMD values for optimizing FD and SD based on batch approximation are consistently higher than those based on the reparameterization trick. In terms of capturing the marginal mode accurately, SDb and BaM are comparable to KLD for the German credit data, and better than KLD for the more challenging a4a data. All variational approximations are at least an order of magnitude faster than MCMC, and the speedup is more apparent as the dimension and number of observations increase.

7.2 Generalized linear mixed models

Let $y_i = (y_{i1}, \ldots, y_{in_i})^\top$ denote the n_i observations for the ith subject and $y = (y_1^\top, \ldots, y_n^\top)^\top$. Each y_{ij} is distributed according to a density in the exponential family, and a smooth invertible link function $g(\cdot)$ relates its mean μ_{ij} to a linear predictor η_{ij} such that

$$g(\mu_{ij}) = \eta_{ij} = X_{ij}^\top \beta + Z_{ij}^\top b_i$$

for $i = 1, \ldots, n$, $j = 1, \ldots, n_i$. Here, $\beta \in \mathbb{R}^p$ is the fixed effect, $b_i \in \mathbb{R}^r$ is the random effect characterizing the ith

subject, and $X_{ij} \in \mathbb{R}^p$ and $Z_{ij} \in \mathbb{R}^r$ are the covariates. We assume $b_i \sim \mathrm{N}(0, G^{-1})$ and let $G = WW^\top$ be the Cholesky decomposition of precision matrix G, where W is a lower triangular matrix with positive diagonal entries. For unconstrained optimization of W, we introduce W^* such that $W_{ii}^* = \log(W_{ii})$ and $W_{ij}^* = W_{ij}$ if $i \neq j$, and let $\zeta = \mathrm{vech}(W^*)$. Normal priors, $\beta \sim \mathrm{N}(0, \sigma_0^2 I_p)$ and $\zeta \sim N(0, \sigma_0^2 I_{r(r+1)/2})$, where $\sigma_0^2 = 100$ are assigned. The global variables are $\theta_G = (\beta^\top, \zeta^\top)^\top$ and the local variables are $\theta_L = (b_1^\top, \ldots, b_n^\top)^\top$. Focusing on GLMMs with canonical links and the one-parameter exponential family, the log joint density of the model can be written as

$$\log h(\theta) = \sum_{i=1}^{n} \sum_{j=1}^{n_i} \log p(y_{ij} | \beta, b_i) + \sum_{i=1}^{n} \log p(b_i | \zeta)$$

$$+ \log p(\beta) + \log p(\zeta)$$

$$= \sum_{i,j} \{y_{ij} \eta_{ij} - A(\eta_{ij})\} + n \log |W|$$

$$- \frac{1}{2} \sum_{i=1}^{n} b_i^\top WW^\top b_i - \frac{\beta^\top \beta}{2\sigma_\beta^2} - \frac{\zeta^\top \zeta}{2\sigma_\zeta^2} + C,$$

where $A(\cdot)$ is the log-partition function and C is a constant independent of θ. For instance, $A(x) = \log(1 + e^x)$ for Bernoulli-distributed binary responses and $A(x) = \exp(x)$ for Poisson-distributed count responses. Let $H = \nabla_\theta^2 \log h(\theta)$ and $H_{\theta_i, \theta_j} = \nabla_{\theta_i, \theta_j}^2 \log h(\theta)$. The Hessian,

$$H = \begin{bmatrix} H_{b_1, b_1} & \cdots & 0 & H_{b_1, \theta_G} \\ \vdots & \ddots & \vdots & \vdots \\ 0 & \cdots & H_{b_n, b_n} & H_{b_n, \theta_G} \\ H_{\theta_G, b_1} & \cdots & H_{\theta_G, b_n} & H_{\theta_G} \end{bmatrix},$$

has a sparse structure similar to Ω. Both $\nabla_\theta h(\theta)$ and H are derived in the supplement.

First, consider the epilepsy data (Thall and Vail, 1990) from a clinical trial with $n = 59$ patients, who were randomly assigned to a drug, progabide (Trt = 1), or a placebo (Trt = 0). The response is the number of seizures experienced by each patient during four follow-up periods. Covariates include logarithm of the patient's age at baseline, which is centered by subtracting the mean (Age), logarithm of 1/4 the number of seizures prior to the trial (Base), visit number coded as -0.3, -0.1, 0.1, 0.3 (Visit), and an indicator of the 4th visit (V4). We consider Poisson mixed models with random intercepts and slopes (Breslow and Clayton, 1993),

$$\text{Epi I}: \log \mu_{ij} = \beta_0 + \beta_{\text{Base}}\text{Base}_i + \beta_{\text{Trt}}\text{Trt}_i + \beta_{\text{Age}}\text{Age}_i$$
$$+ \beta_{\text{BaseTrt}}\text{Base}_i\text{Trt}_i + \beta_{\text{V4}}\text{V4}_{ij} + b_i,$$

$$\text{Epi II}: \log \mu_{ij} = \beta_0 + \beta_{\text{Base}}\text{Base}_i + \beta_{\text{Trt}}\text{Trt}_i + \beta_{\text{Age}}\text{Age}_i$$
$$+ \beta_{\text{BaseTrt}}\text{Base}_i\text{Trt}_i + \beta_{\text{Visit}}\text{Visit}_{ij} + b_{i1} + b_{i2}\text{Visit}_{ij},$$

for $i = 1, ..., n$, $j = 1, ..., 4$.

Next, consider the toenail data (De Backer et al., 1998) from a clinical trial comparing two oral antifungal treatments for toenail infections. Each of 294 patients was evaluated for up to seven visits, resulting in a total of 1908 observations. Patients were randomized to receive 250 mg of terbinafine (Trt = 1) or 200 mg of itraconazole (Trt = 0) per day. The response variable is binary, with 0 indicating no or mild nail separation and 1 for moderate or severe separation. Visit times in months (t) are standardized to have mean 0 and variance 1. A logistic random intercept model is fitted to this data,

$$\text{logit}(\mu_{ij}) = \beta_0 + \beta_{\text{Trt}}\text{Trt}_i + \beta_t t_{ij} + \beta_{\text{Trt}\times t}\text{Trt}_i \times t_{ij} + b_i,$$

for $i = 1, ..., 294, 1 \le j \le 7$.

Lastly, we analyze the polypharmacy data (Hosmer et al., 2013) which contains 500 subjects, each observed for drug usage over 7 years, resulting in 3500 binary responses. Covariates include Gender (1 for males, 0 for females), Race (0 for whites, 1 otherwise), Age ($\log(\text{age}/10)$) and INPTMHV (0 if there are no inpatient mental health visits and 1 otherwise). The number

of outpatient mental health visits (MHV) is coded using MHV1 = 1 if $1 \le \text{MHV} \le 5$, MHV2 = 1 if $6 \le \text{MHV} \le 14$, and MHV3 = 1 if $\text{MHV} \ge 15$. We consider a logistic random intercept model,

$$\text{logit}(\mu_{ij}) = \beta_0 + \beta_{\text{Gender}}\text{Gender}_i + \beta_{\text{Race}}\text{Race}_i$$
$$+ \beta_{\text{Age}}\text{Age}_{ij} + \beta_{\text{MHV1}}\text{MHV1}_{ij} + \beta_{\text{MHV2}}\text{MHV2}_{ij}$$
$$+ \beta_{\text{MHV3}}\text{MHV3}_{ij} + \beta_{\text{INPT}}\text{INPTMHV}_{ij} + b_i,$$

for $i = 1, \ldots, 500, j = 1, \ldots, 7$.

In this section, we use batch size $B = 5$ for FDb and SDb. For BAM, $B = 100$ for the epilepsy data and $B = 1000$ for the toenail and polypharmacy data. A larger batch size is used in the latter cases as BAM is very prone to ill-conditioned updates and the convergence is very slow for smaller batch sizes. The maximum number of iterations for the epilepsy data is $60,000$, and reduced to $30,000$ for the toenail and polypharmacy data as they contain much more observations.
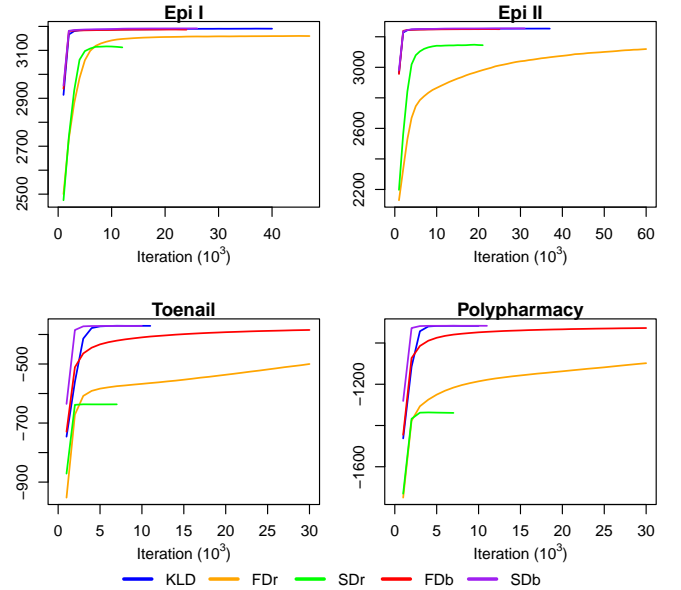

Fig 7: GLMMs: Average lower bound every 1000 iterations.

Fig 7 shows that SDb is among the fastest to converge among SGD methods, achieving a lower bound higher than KLD for Epi I, Epi II and polypharmacy, and comparable to KLD for toenail. While FDb converges rapidly for Epi I and Epi II, it fails to converge by the maximum iteration of 30,000 for toenail and polypharmacy. Overall,

		KLD	FDr	SDr	FDb	SDb	BaM	MCMC
MMD	Epi I	6.37±0.19	0.04±0.02	-0.06±0.02	2.89±0.05	6.48±0.22	9.51±1.52	-
	Epi II	6.34±0.13	0.04±0.03	0.06±0.03	4.65±0.05	5.97±0.17	6.41±0.22	-
	Toenail	4.17±0.05	0.35±0.01	0.11±0.01	1.42±0.01	2.53±0.02	2.46±0.02	-
	Polypharmacy	5.66±0.05	0.49±0.00	0.19±0.01	2.40±0.01	3.79±0.03	3.80±0.03	-
$\frac{\|\mu-\mu^*\|}{\sigma^*}$	Epi I	0.07±0.05	2.04±1.62	2.30±2.09	0.28±0.19	0.07±0.05	0.07±0.05	-
	Epi II	0.09±0.07	2.14±1.79	2.55±2.40	0.19±0.16	0.09±0.08	0.09±0.07	-
	Toenail	0.21±0.14	1.20±1.30	1.57±2.17	0.68±0.65	0.36±0.20	0.38±0.22	-
	Polypharmacy	0.18±0.10	1.01±1.19	1.34±2.12	0.44±0.38	0.22±0.13	0.23±0.13	-
$\frac{\sigma}{\sigma^*}$	Epi I	0.95±0.06	0.76±0.26	0.72±0.34	0.81±0.21	0.94±0.05	0.99±0.02	-
	Epi II	0.94±0.08	0.94±0.29	0.69±0.28	0.88±0.18	0.95±0.08	0.97±0.07	-
	Toenail	0.87±0.05	0.35±0.14	0.10±0.05	0.66±0.13	0.76±0.11	0.75±0.12	-
	Polypharmacy	0.94±0.03	0.39±0.12	0.13±0.05	0.80±0.09	0.86±0.07	0.86±0.07	-
time	Epi I	2.3 (40)	16.7 (47)	4.3 (12)	6.6 (24)	8.9 (26)	0.8 (0.3)	95.9
	Epi II	3.9 (37)	73.3 (60)	26.0 (21)	16.7 (25)	28.5 (31)	13.1 (1.55)	380.8
	Toenail	2.8 (11)	117.4 (30)	27.7 (7)	93.7 (30)	35.0 (10)	32.5 (0.3)	171.1
	Polypharmacy	5.1 (10)	346.1 (30)	94.7 (7)	285.8 (30)	131.8 (11)	112.5 (0.4)	506.2

TABLE 7

GLMMs: Estimates of mean and standard deviation for MMD, normalized absolute difference in mode and standard deviation ratio. Runtime is in seconds and number of iterations (in thousands) is given in brackets.

methods based on FD (FDr, FDb) seem to converge much more slowly than methods based on SD (SDr, SDb).

From the MMD results in Table 7, FDr and SDr have the lowest MMD. In contrast, FDb and SDb yield substantial improvements over their reparameterization trick-based counterparts, achieving much higher MMDs. Among SGD methods based on the weighted Fisher divergence, SDb has the highest MMD, even surpassing KLD for Epi I. BaM outperforms KLD for Epi I and Epi II, but its performance falters for toenail and polypharmacy, where the dimension of θ is higher, reflecting the challenges that BaM faces in high-dimensional cases.

KLD is able to capture the marginal posterior mode of each variable most accurately, with comparable performance from SDb and BaM. While BaM captured the marginal posterior variance most accurately for Epi I and Epi II, its performance falls behind KLD for the higher-dimensional toenail and polypharmacy data. SDr underestimates the marginal posterior variance most severely, which is reminiscent of the "variational collapse" problem it faces in the mean-field setting.

BaM is able to converge using the least number of iterations, by leveraging on closed-form updates and larger batch sizes. However, the computation cost per iteration of BaM is much higher than SGD methods, which can exploit the sparse structure of the precision matrix. This issue becomes more apparent as the dimension of θ increases. Among SGD methods, the runtime of KLD is the shortest. Methods based on FD tend to require more iterations to converge than those based on SD, resulting in longer runtime. SDb is able to converge in approximately the same number of iterations as KLD, although each iteration takes longer.

Fig 8 compares the marginal densities estimated using MCMC with variational approximations from KLD, SDb, and BaM for some variables in Epi I and polypharmacy. For Epi I in the first row, all variational approaches match the MCMC results very closely except for ζ, where SDb underestimated the marginal posterior variance more severely than BaM and KLD. For the higher dimensional polypharmacy data in the second row, KLD matches the MCMC results most closely, while SDb and BaM display a higher tendency to underestimate the marginal posterior variance although the mode was captured more accurately in some cases.
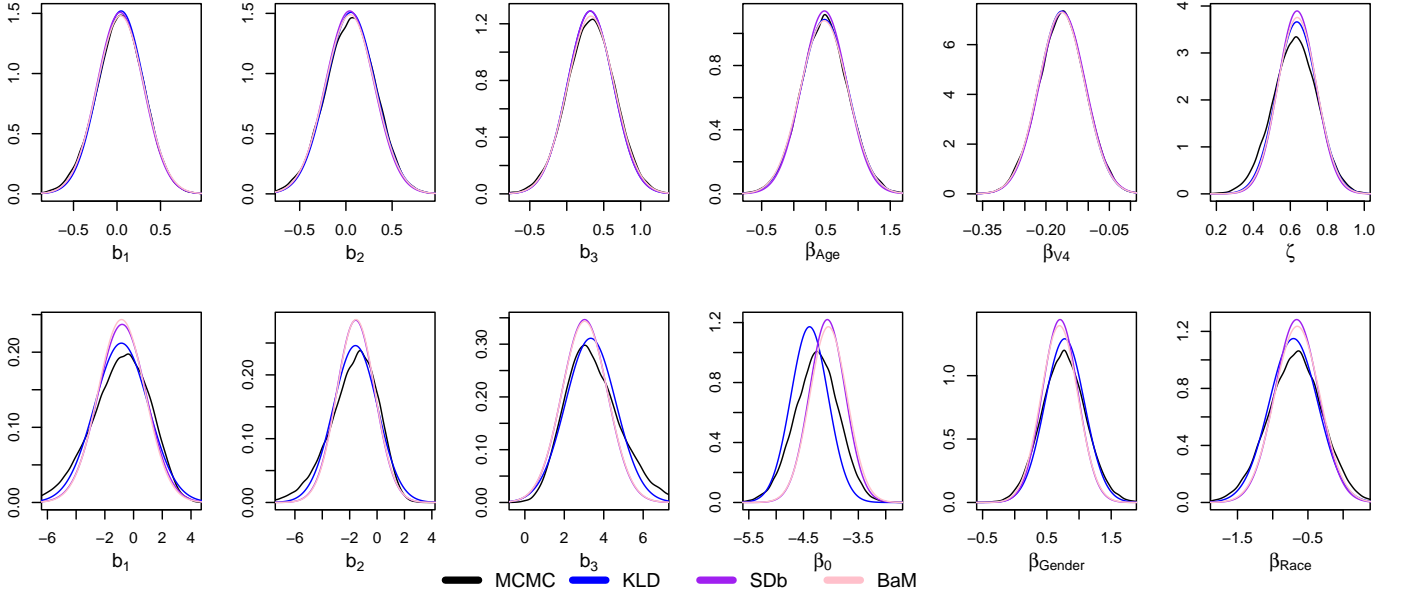
19

Fig 8: Marginal density estimates for some local and global variables in Epi I (first row) and polypharmacy (second row).

7.3 Stochastic volatility models

The stochastic volatility model is widely used to capture the dynamic nature of financial time series. It provides an attractive alternative to constant volatility models like the Black-Scholes model (Black and Scholes, 1973), as the volatility of asset returns evolves over time according to a stochastic process. The response at time t is

$$y_t \sim \mathrm{N}(0, \exp(\lambda + \sigma b_t)) \quad \text{for} \quad t = 1, \ldots, n,$$

where $\lambda \in \mathbb{R}$, $\sigma > 0$, and the latent volatility process b_t follows an autoregressive model of order one such that

$$b_t \sim \mathrm{N}(\phi b_{t-1}, 1) \text{ for } t = 2, \ldots, n,$$

$$b_1 \sim \mathrm{N}(0, 1/(1 - \phi^2)),$$

where $\phi \in (0, 1)$. To allow unconstrained updates, we apply the transformations, $\sigma = \exp(\alpha)$ and $\phi = \{\exp(-\psi) + 1\}^{-1}$. The set of local variables are $\theta_L = (b_1, \ldots, b_n)^\top$ and the set of global variables are $\theta_G = (\alpha, \lambda, \psi)^\top$. We consider the prior $\theta_G \sim \mathrm{N}(0, \sigma_0^2 I)$, where $\sigma_0^2 = 10$. For this model, b_i is independent of b_j given θ_G a posteriori if $|i - j| > 1$. The log joint density is

$$\log h(\theta) = -\frac{n\lambda}{2} - \frac{\sigma}{2} \sum_{t=1}^{n} b_t - \frac{1}{2} \sum_{t=1}^{n} y_t^2 \exp\{-\lambda - \sigma b_t\}$$

$$- \frac{1}{2} \sum_{t=2}^{n} (b_t - \phi b_{t-1})^2 + \frac{1}{2} \log(1 - \phi^2)$$

$$- \frac{1}{2} b_1^2 (1 - \phi^2) - \frac{\alpha^2}{2\sigma_0^2} - \frac{\lambda^2}{2\sigma_0^2} - \frac{\psi^2}{2\sigma_0^2} + C,$$

where C is a constant independent of θ. The gradient $\nabla_\theta h(\theta)$ and the Hessian,

$$\nabla_\theta^2 \log h(\theta) = \begin{bmatrix} H_{b_1,b_1} & H_{b_1,b_2} & \ldots & 0 & H_{b_1,\theta_G} \\ H_{b_2,b_1} & H_{b_2,b_2} & \ldots & 0 & H_{b_2,\theta_G} \\ \vdots & \vdots & \ddots & \vdots & \vdots \\ 0 & 0 & \ldots & H_{b_n,b_n} & H_{b_n,\theta_G} \\ H_{\theta_G,b_1} & H_{\theta_G,b_2} & \ldots & H_{\theta_G,b_n} & H_{\theta_G,\theta_G} \end{bmatrix},$$

which has the same sparsity structure as Ω in the variational approximation, are derived in the supplement.

We analyze two datasets from `Garch` in the R package `Ecdat`. The first contains $n = 945$ observations of the weekday exchange rates of the U.S. Dollar against the British Pound (GBP) from 1 Oct 1981 to 28 June 1985. The second contains $n = 1866$ observations of the weekday exchange rates for the U.S. Dollar against the German Deutschemark (DEM) from 2 Jan 1980 to 21 June 1987. For both datasets, the mean-corrected log-return series $\{y_t\}$ is derived from exchange rates $\{r_t\}$ using

$$y_t = 100 \times \left\{ \log\left(\frac{r_t}{r_{t-1}}\right) - \frac{1}{n} \sum_{i=1}^{n} \log\left(\frac{r_i}{r_{i-1}}\right) \right\}.$$

We use $B = 10$ for FDb and SDb, while BaM is executed with $B = 50$ for GBP. We have tried larger batch sizes

		KLD	FDr	SDr	FDb	SDb	BaM	MCMC
MMD	GBP	3.83±0.09	0.45±0.01	1.03±0.01	0.49±0.01	3.26±0.08	3.59±0.09	-
	DEM	5.34 ± 0.27	0.36 ± 0.01	0.78 ± 0.01	0.40 ± 0.01	6.02 ± 0.15	-	-
$\frac{\lvert\mu-\mu^*\rvert}{\sigma^*}$	GBP	0.07±0.05	0.43±0.43	0.36±0.32	0.38±0.37	0.04±0.03	0.05±0.04	-
	DEM	0.09±0.07	1.15±0.91	1.19±0.74	0.99±0.77	0.06±0.05	-	-
time	GBP	7.1 (27)	12.7 (30)	6.6 (15)	621.8 (30)	419.2 (16)	1521.5 (3.25)	3573.2
	DEM	9.7 (19)	27.3 (30)	23.7 (25)	2748.0 (30)	1281.3 (11)	-	5764.9

TABLE 8

SSMs: Estimates of mean and standard deviation for MMD and normalized absolute difference in mode. Runtime is in seconds and number of iterations (in thousands) is given in brackets.

for BaM, but these resulted in severely ill-conditioned updates. For the higher-dimensional DEM, we cannot get BaM to converge despite trying various batch sizes. The challenge of inferring a full covariance matrix of order $d = 1869$ for BaM here is immense, not to mention the computational cost of inverting matrices of this order. The maximum number of iterations is set as $30,000$.

From the MMD values in Table 8, FDr, SDr and FDb perform very poorly, compared to the rest. SDb yields the best performance among SGD methods optimizing the weighted Fisher divergence. Its MMD values are close to those of KLD for GBP, and even surpass KLD for the higher-dimensional DEM. SDb and BaM are also able to capture the mode more accurately than KLD for both datasets. In terms of runtime, KLD is the most efficient approach, attaining very high MMD values with the shortest runtime. While BaM requires fewer iterations to converge, the computational cost per iteration is much higher, leading to long runtimes. For instance, BaM requires 1521 seconds to converge for GBP, which is nearly triple the runtime of SDb. As the dimensionality increases, BaM also becomes more unstable and prone to ill-conditioned updates making convergence very difficult, while SDb provides a more reliable and computationally feasible approach for optimizing the batch approximated SD.

Fig 9 presents the impact of varying the batch size for SDb in terms of the rate of convergence and quality of approximation measured by MMD. Increasing the batch size clearly leads to faster convergence and improved approximation quality. The total runtime as shown in the legends of the first row of Fig 9 is also reduced as lesser number of
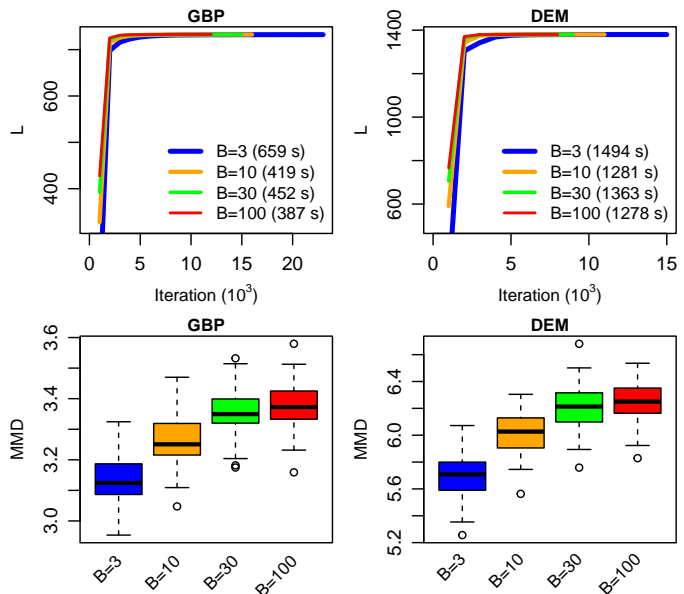

Fig 9: SSMs: Average lower bound over every 1000 iterations and boxplot of MMD values for different batch sizes for SDb.

iterations is required for convergence. This suggests that larger batch sizes can enhance both the stability and accuracy of SDb.

Fig 10 shows the marginal posterior density estimates from MCMC, KLD and SDb ($B = 10, 100$) for some local variables and all the global variables from DEM. SDb can capture the marginal posterior mode more accurately than KLD, especially for each of the global variables, but has a higher tendency to underestimate the posterior variance. Increasing the batch size from 10 to 100 helps in reducing underestimation of the posterior variance.
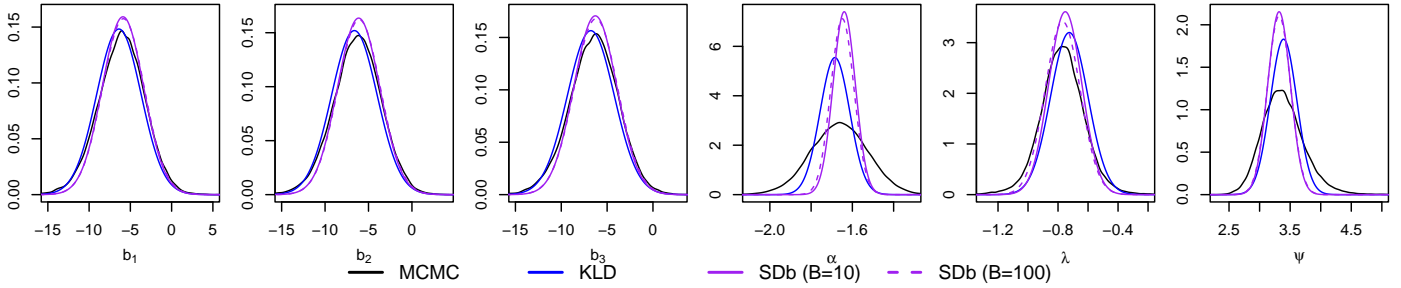
Fig 10: Marginal density estimates for some local and global variables in DEM.

8. CONCLUSION

In this article, we evaluate the performance of Gaussian variational inference based on the weighted Fisher divergence by focusing on the FD and SD. First, we consider the mean-field assumption for both Gaussian and non-Gaussian targets. We demonstrate that FD and SD tend to underestimate the posterior variance more severely than KLD for Gaussian targets in this context. SD has the potential to capture the posterior mode more accurately than FD and KLD for skewed targets, but underestimates the variance more severely.

Next, we consider high-dimensional hierarchical models for which posterior conditional independence structure can be captured using a sparse precision matrix in the Gaussian variational approximation. To impose sparsity on the Cholesky factor of the precision matrix, we consider optimization based on SGD and propose two approaches based on the reparametrization trick and a batch approximation of the objective.

The reparametrization trick yields unbiased gradient estimates but involves a Hessian matrix, which can be computationally expensive and increases variability in the gradients, leading to reduced stability and slow convergence. To address these issues, we introduce an alternative that minimizes a biased estimate of the FD and SD using a random batch of samples at each iteration. This eliminates reliance on the Hessian matrix, improving stability. This approach can also be interpreted as optimizing a new objective that iteratively improves the match between gradients of the posterior and variational density, at sample points that shift gradually towards high prob-

ability regions of the posterior. We evaluate the behavior of this new objective under the mean-field assumption for Gaussian targets and show that it alleviates the variational collapse issue faced previously by SD.

The proposed methods are compared to KLD and BaM in applications involving logistic regression, GLMMs and stochastic volatility models. Extensive experiments reveal that FDr and SDr converge very slowly, often to suboptimal variational approximations. FDb and SDb provide substantial improvements over FDr and SDr, with SDb having superior performance in terms of convergence rate and quality of variational approximation attained. BaM, which relies on closed-form updates and hence requires fewer iterations to converge, is very effective for logistic regression. However, it is much less efficient than KLD for GLMMs and SSMs, and its performance gradually worsens as the dimension increases, eventually failing to converge. SDb has an advantage over BaM in high dimensions as it is able to impose sparsity on the precision matrix, remains feasible computationally and is more stable and less sensitive to poor initialization. SDb can also capture posterior modes more accurately than KLD although it is more prone to variance underestimation.

Several avenues for future research remain open. Our analysis focused on Gaussian variational approximations for FD and SD, and it will be valuable to investigate the performance of FD and SD under more flexible variational families. While we have used SGD for optimization, the choice of optimizer and associated hyperparameters significantly influences convergence behavior, and it will be useful to explore alternative optimization techniques that do not rely on SGD. Our findings also high-

light the potential of the batch approximated SD, and it will be interesting to further investigate its properties in other contexts.

FUNDING

REFERENCES

Agrawal, A. and J. Domke (2024). Disentangling impact of capacity, objective, batchsize, estimators, and step-size on flow VI. *arXiv preprint arXiv:2412.08824*.

Barp, A., F.-X. Briol, A. B. Duncan, M. Girolami, and L. Mackey (2019). Minimum Stein discrepancy estimators. In H. Wallach, H. Larochelle, A. Beygelzimer, F. d'Alché Buc, E. Fox, and R. Garnett (Eds.), *Advances in Neural Information Processing Systems*, Volume 32, pp. 12964–12976. Curran Associates, Inc.

Black, F. and M. Scholes (1973). The pricing of options and corporate liabilities. *Journal of political economy 81*, 637–654.

Blei, D. M., A. Kucukelbir, and J. D. McAuliffe (2017). Variational inference: A review for statisticians. *Journal of the American Statistical Association 112*, 859–877.

Breslow, N. E. and D. G. Clayton (1993). Approximate inference in generalized linear mixed models. *Journal of the American Statistical Association 88*, 9–25.

Cai, D., C. Modi, C. C. Margossian, R. M. Gower, D. M. Blei, and L. K. Saul (2024). EigenVI: Score-based variational inference with orthogonal function expansions. In S. Shalev-Shwartz, A. Shashua, G. Chechik, G. Elidan, and B. Nadler (Eds.), *Advances in Neural Information Processing Systems*, Volume 37, pp. 12345–12356. Curran Associates, Inc.

Cai, D., C. Modi, L. Pillaud-Vivien, C. C. Margossian, R. M. Gower, D. M. Blei, and L. K. Saul (2024). Batch and match: Black-box variational inference with a score-based divergence. In K. Chaudhuri and R. Salakhutdinov (Eds.), *Proceedings of the 41st International Conference on Machine Learning*, Volume 202, pp. 1234–1245. PMLR.

De Backer, M., C. De Vroey, E. Lesaffre, I. Scheys, and P. D. Keyser (1998). Twelve weeks of continuous oral therapy for toenail onychomycosis caused by dermatophytes: A double-blind comparative trial of terbinafine 250 mg/day versus itraconazole 200 mg/day. *Journal of the American Academy of Dermatology 38*, 57–63.

Dinh, L., J. Sohl-Dickstein, and S. Bengio (2017). Density estimation using real NVP. In Y. Bengio and Y. LeCun (Eds.), *5th International Conference on Learning Representations*. OpenReview.

Durante, D. and T. Rigon (2019). Conditionally conjugate mean-field variational Bayes for logistic models. *Statistical Science 34*, 472 – 485.

Durrett, R. (2019). *Probability: Theory and Examples* (5th ed.). Cambridge: Cambridge university press.

Elkhalil, K., A. Hasan, J. Ding, S. Farsiu, and V. Tarokh (2021). Fisher auto-encoders. In A. Banerjee and K. Fukumizu (Eds.), *Proceedings of The 24th International Conference on Artificial Intelligence and Statistics*, Volume 130, pp. 352–360. PMLR.

Giordano, R., T. Broderick, and M. I. Jordan (2018). Covariances, robustness, and variational Bayes. *Journal of machine learning research 19*, 1–49.

Hoffman, M. and D. Blei (2015). Stochastic structured variational inference. In G. Lebanon and S. Vishwanathan (Eds.), *Proceedings of the 18th International Conference on Artificial Intelligence and Statistics*, Volume 38, pp. 361–369. PMLR.

Hosmer, D. W., S. Lemeshow, and R. X. Sturdivant (2013). *Applied Logistic Regression* (3rd ed.). Hoboken, NJ: John Wiley & Sons, Inc.

Huggins, J. H., M. Kasprzak, T. Campbell, and T. Broderick (2020). Validated variational inference via practical posterior error bounds. In S. Chiappa and R. Calandra (Eds.), *Proceedings of the 23rd International Conference on Artificial Intelligence and Statistics*, Volume 108, pp. 1792–1802. PMLR.

Hyvärinen, A. (2005). Estimation of non-normalized statistical models by score matching. *Journal of Machine Learning Research 6*, 695–709.

Kingma, D. P. and M. Welling (2014). Auto-encoding variational Bayes. In Y. Bengio and Y. LeCun (Eds.), *2nd International Conference on Learning Representations*. OpenReview.

Li, Y. and R. E. Turner (2016). Rényi divergence variational inference. In D. Lee, M. Sugiyama, U. Luxburg, I. Guyon, and R. Garnett (Eds.), *Advances in Neural Information Processing Systems*, Volume 29, pp. 1073–1081. Curran Associates, Inc.

Liu, Q. and D. Wang (2016). Stein variational gradient descent: A general purpose bayesian inference algorithm. In D. D. Lee, M. Sugiyama, U. V. Luxburg, I. Guyon, and R. Garnett (Eds.), *Advances in Neural Information Processing Systems*, Volume 29, pp. 2378–2386. Curran Associates, Inc.

Maclaurin, D. and R. P. Adams (2015). Firefly monte carlo: Exact mcmc with subsets of data. In Q. Yang and M. Wooldridge (Eds.), *Proceedings of the 24th International Joint Conference on Artificial Intelligence*, pp. 4289–4295. AAAI Press.

Margossian, C. C., L. Pillaud-Vivien, and L. K. Saul (2024). Variational inference for uncertainty quantification: An analysis of trade-offs. In G. Camps-Valls, F. J. R. Ruiz, and I. Valera (Eds.), *Proceed-

ings of the 27th International Conference on Artificial Intelligence and Statistics, Volume 206, pp. 1234–1245. PMLR.

Modi, C., C. Margossian, Y. Yao, R. Gower, D. Blei, and L. Saul (2023). Variational inference with Gaussian score matching. In S. Shalev-Shwartz, A. Shashua, G. Chechik, G. Elidan, and B. Nadler (Eds.), *Advances in Neural Information Processing Systems*, Volume 36, pp. 1073–1081. Curran Associates, Inc.

O'Donoghue, B., E. Chu, N. Parikh, and S. Boyd (2016). Conic optimization via operator splitting and homogeneous self-dual embedding. *Journal of Optimization Theory and Applications 169*, 1042–1068.

Ormerod, J. T. and M. P. Wand (2010). Explaining variational approximations. *The American Statistician 64*, 140–153.

Ranganath, R., D. Tran, and D. M. Blei (2016). Hierarchical variational models. In M. F. Balcan and K. Q. Weinberger (Eds.), *Proceedings of The 33rd International Conference on Machine Learning*, Volume 37, pp. 324–333. PMLR.

Rezende, D. J., S. Mohamed, and D. Wierstra (2014). Stochastic backpropagation and approximate inference in deep generative models. In E. P. Xing and T. Jebara (Eds.), *Proceedings of The 31st International Conference on Machine Learning*, Volume 32, pp. 1278–1286. PMLR.

Robert, C. P. and G. Casella (2004). *Monte Carlo Statistical Methods* (2nd ed.). New York: Springer-Verlag.

Rothman, A. J., E. Levina, and J. Zhu (2010). Sparse multivariate regression with covariance estimation. *Journal of Computational and Graphical Statistics 19*, 947–962.

Sha, F., Y. Lin, L. K. Saul, and D. D. Lee (2003). Multiplicative updates for nonnegative quadratic programming in support vector machines. In S. Becker, S. Thrun, and K. Obermayer (Eds.), *Advances in Neural Information Processing Systems*, Volume 15, pp. 897–904. MIT Press.

Tan, L. S. L. (2021). Use of model reparametrization to improve variational Bayes. *Journal of the Royal Statistical Society Series B: Statistical Methodology 83*, 30–57.

Tan, L. S. L. and A. Chen (2024). Variational inference based on a subclass of closed skew normals. *Journal of Computational and Graphical Statistics* (to appear).

Tan, L. S. L. and D. J. Nott (2018). Gaussian variational approximation with sparse precision matrices. *Statistics and Computing 28*, 259–275.

Thall, P. F. and S. C. Vail (1990). Some covariance models for longitudinal count data with overdispersion. *Biometrics 46*, 657–671.

Yang, Y., R. Martin, and H. Bondell (2019). Variational approximations using Fisher divergence. arXiv: 1905.05284.

Yu, L. and C. Zhang (2023). Semi-implicit variational inference via score matching. In Y. Liu (Ed.), *Proceedings of the 11th International Conference on Learning Representations*. OpenReview.

Zeiler, M. D. (2012). Adadelta: An adaptive learning rate method. arXiv: 1212.5701.

Zhou, J., J. T. Ormerod, and C. Grazian (2023). Fast expectation propagation for heteroscedastic, lasso-penalized, and quantile regression. *Journal of Machine Learning Research 24*, 1–39.

Supplementary Material

S1. UNIVARIATE NON-GAUSSIAN TARGET

We begin by deriving some key expressions that will be used throughout our analysis of non-Gaussian target distributions. We assume the variational approximation $q(\theta) = \phi(\theta|\mu,\sigma^2)$. Its log-density and gradient are

$$\log q(\theta) = -\frac{1}{2}\log(2\pi) - \frac{1}{2}\log(\sigma^2) - \frac{(\theta-\mu)^2}{2\sigma^2},$$

$$\nabla_\theta \log q(\theta) = -\frac{\theta-\mu}{\sigma^2}.$$

The expectation of $\log q(\theta)$ with respect to $q(\theta)$ is

$$\mathrm{E}_q\left\{\log q(\theta)\right\} = -\frac{1}{2}\log(2\pi\sigma^2) - \frac{1}{2}.$$

S1.1 Student's t

The log-density and its gradient for $\theta \sim t(\nu)$ are

$$\log p(\theta,y) = \log\left\{\Gamma\left(\frac{\nu+1}{2}\right)\right\} - \frac{1}{2}\log(\pi\nu)$$
$$- \log\left\{\Gamma\left(\frac{\nu}{2}\right)\right\} - \frac{\nu+1}{2}\log\left(1+\frac{\theta^2}{\nu}\right),$$

$$\nabla \log p(\theta,y) = -(\nu+1)\frac{\theta}{\nu+\theta^2},$$

where ν is the degree of freedom. The evidence lower bound for KLD is

$$\mathcal{L} = \mathrm{E}_q\left\{\log p(\theta,y) - \log q(\theta)\right\}$$
$$= \log\left\{\Gamma\left(\frac{\nu+1}{2}\right)\right\} - \frac{1}{2}\log(\pi\nu) - \log\left\{\Gamma\left(\frac{\nu}{2}\right)\right\}$$
$$- \frac{\nu+1}{2}\mathrm{E}_q\log\left(1+\frac{\theta^2}{\nu}\right) + \frac{1}{2}\log(2\pi\sigma^2) + \frac{1}{2}.$$

The Fisher divergence is

$$F(q\|p) = \mathrm{E}_q\{\|\nabla_\theta \log p(\theta,y) - \nabla_\theta \log q(\theta)\|^2\}$$

$$= \mathrm{E}_q\left\{\left\|-(\nu+1)\frac{\theta}{\nu+\theta^2} + \frac{\theta-\mu}{\sigma^2}\right\|^2\right\}$$

$$= (\nu+1)^2 \mathrm{E}_q\left\{\frac{\theta^2}{(\nu+\theta^2)^2}\right\} + \mathrm{E}_q\left\{\frac{(\theta-\mu)^2}{\sigma^4}\right\}$$

$$- 2\frac{\nu+1}{\sigma^2}\mathrm{E}_q\left\{\frac{\theta(\theta-\mu)}{\nu+\theta^2}\right\}$$

$$= (\nu+1)^2 \mathrm{E}_q\left\{\frac{\theta^2}{(\nu+\theta^2)^2}\right\} + \frac{1}{\sigma^2}$$

$$- \frac{2(\nu+1)}{\sigma^2}\mathrm{E}_q\left\{\frac{\theta(\theta-\mu)}{\nu+\theta^2}\right\}.$$

S1.2 Log transformed inverse Gamma

For the log transformed inverse gamma, let $a_1 = a_0 + n/2$ and $b_1 = b_0 + \sum_{i=1}^{n} y_i^2/2$. Then its log-density and gradient are given by

$$\log p(y,\theta) = -\frac{n}{2}\log(2\pi) + a_0 \log b_0 - \log\Gamma(a_0)$$
$$- a_1\theta - b_1\exp(-\theta),$$

$$\nabla_\theta \log p(y,\theta) = -a_1 + b_1\exp(-\theta).$$

Taking the expectation of $\log p(y,\theta)$ with respect to $q(\theta)$,

$$\mathrm{E}_q\left\{\log p(y,\theta)\right\} = -\frac{n}{2}\log(2\pi) + a_0\log b_0 - \log\Gamma(a_0)$$
$$- a_1\mu - \exp\left(\frac{\sigma^2}{2} - \mu\right)b_1.$$

Hence, the evidence lower bound for KLD is

$$\mathcal{L} = \mathrm{E}_q\left\{\log p(y,\theta) - \log q(\theta)\right\}$$
$$= -\frac{n}{2}\log(2\pi) + a_0\log b_0 - \log\Gamma(a_0) - a_1\mu$$
$$- \exp\left(\frac{\sigma^2}{2} - \mu\right)b_1 + \frac{1}{2}\log(2\pi\sigma^2) + \frac{1}{2}.$$

For the Fisher divergence, we evaluate the expectation of the squared norm of the gradient difference,

$$F(q\|p) = \mathrm{E}_q\{\|\nabla_\theta \log p(y,\theta) - \nabla_\theta \log q(\theta)\|^2\}$$

$$= \mathrm{E}_q\left\{\left\|-a_1 + \exp(-\theta)b_1 + \frac{\theta-\mu}{\sigma^2}\right\|^2\right\}$$

$$= a_1^2 + b_1^2\mathrm{E}_q\left\{\exp(-2\theta)\right\} + \mathrm{E}_q\left\{\frac{(\theta-\mu)^2}{\sigma^4}\right\}$$

$$- 2a_1 b_1\mathrm{E}_q\left\{\exp(-\theta)\right\} - 2a_1\mathrm{E}_q\left\{\frac{\theta-\mu}{\sigma^2}\right\}$$

$$+ 2b_1\mathrm{E}_q\left\{\exp(-\theta)\frac{\theta-\mu}{\sigma^2}\right\}.$$

Note that $\mathrm{E}_q\{\exp(-a\theta)\} = \exp(a^2\sigma^2/2 - a\mu)$ for any constant $a \in \mathbb{R}$. Thus,

$$F(q\|p) = a_1^2 + b_1^2\exp(2\sigma^2 - 2\mu)$$
$$- 2b_1(a_1+1)\exp(\sigma^2/2 - \mu) + 1/\sigma^2.$$

We have

$$S(q\|p) = \sigma^2 F(q\|p)$$
$$= \sigma^2\{a_1^2 + b_1^2\exp(2\sigma^2 - 2\mu)$$
$$- 2b_1(a_1+1)\exp(\sigma^2/2 - \mu)\} + 1.$$

$$\nabla_\mu S(q\|p) = 2b_1\sigma^2 \exp(\sigma^2/2 - \mu)\{(a_1 + 1)$$
$$- b_1 \exp(3\sigma^2/2 - \mu)\} = 0$$
$$\therefore \mu = \log \frac{b_1}{a_1 + 1} + \frac{3\sigma^2}{2}.$$

At this value of μ,

$$S(q\|p) = a_1^2\sigma^2 - (a_1 + 1)^2\sigma^2 \exp(-\sigma^2) + 1.$$

$$\nabla_{\sigma^2} S(q\|p) = a_1^2 + (a_1 + 1)^2 \exp(-\sigma^2)(\sigma^2 - 1).$$

S1.3 Skew normal

The probability density function (pdf) for $\theta \sim$ SN(m, t, λ) is

$$p(\theta, y) = 2\,\phi(\theta|m, t^2)\,\Phi\{\lambda(\theta - m)\}.$$

The log-density and gradient for the skew normal are

$$\log p(\theta, y) = \log 2 - \frac{1}{2}\log(2\pi t^2) - \frac{(\theta - m)^2}{2t^2}$$
$$+ \log[\Phi\{\lambda(\theta - m)\}],$$

$$\nabla_\theta \log p(\theta, y) = -\frac{\theta - m}{t^2} + \frac{\lambda\phi\{\lambda(\theta - m)\}}{\Phi\{\lambda(\theta - m)\}}.$$

Taking the expectation of $\log p(\theta, y)$ with respect to $q(\theta)$,

$$\mathrm{E}_q\{\log p(\theta, y)\} = \log 2 - \frac{1}{2}\log(2\pi t^2) - \frac{\sigma^2 + (\mu - m)^2}{2t^2}$$
$$+ \mathrm{E}_q \log[\Phi\{\lambda(\theta - m)\}].$$

For KLD, we maximize the evidence lower bound

$$\mathcal{L} = \mathrm{E}_q\{\log p(\theta, y) - \log q(\theta)\}$$
$$= \log 2 - \frac{1}{2}\log(2\pi t^2) - \frac{\sigma^2 + (\mu - m)^2}{2t^2}$$
$$+ \mathrm{E}_q \log[\Phi\{\lambda(\theta - m)\}] + \frac{1}{2}\log(2\pi\sigma^2) + \frac{1}{2}.$$

The Fisher divergence is given by

$$F(q\|p) = \mathrm{E}_q\{\|\nabla_\theta \log p(\theta, y) - \nabla_\theta \log q(\theta)\|^2\}$$
$$= \mathrm{E}_q\left\{\left\| -\frac{\theta - m}{t^2} + \frac{\lambda\phi\{\lambda(\theta - m)\}}{\Phi\{\lambda(\theta - m)\}} + \frac{\theta - \mu}{\sigma^2}\right\|^2\right\}$$
$$= \mathrm{E}_q\left\{\frac{(\theta - m)^2}{t^4}\right\} + 2\,\mathrm{E}_q\left[\frac{\lambda\phi\{\lambda(\theta - m)\}}{\Phi\{\lambda(\theta - m)\}}\frac{(\theta - \mu)}{\sigma^2}\right]$$
$$+ \mathrm{E}_q\left\{\frac{(\theta - \mu)^2}{\sigma^4}\right\} - 2\,\mathrm{E}_q\left[\frac{(\theta - m)}{t^2}\frac{\lambda\phi\{\lambda(\theta - m)\}}{\Phi\{\lambda(\theta - m)\}}\right]$$
$$- 2\,\mathrm{E}_q\left\{\frac{(\theta - m)(\theta - \mu)}{t^2\sigma^2}\right\} + \mathrm{E}_q\left[\frac{\lambda^2\phi^2\{\lambda(\theta - m)\}}{\Phi^2\{\lambda(\theta - m)\}}\right].$$

After computing the 1st, 3rd and 5th terms in the final expression exactly, we obtain

$$F(q\|p) = \frac{\sigma^2 + (\mu - m)^2}{t^4} + \lambda^2 \mathrm{E}_q\left[\frac{\phi^2\{\lambda(\theta - m)\}}{\Phi^2\{\lambda(\theta - m)\}}\right]$$
$$+ \frac{1}{\sigma^2} - \frac{2\lambda}{t^2}\,\mathrm{E}_q\left[(\theta - m)\frac{\phi\{\lambda(\theta - m)\}}{\Phi\{\lambda(\theta - m)\}}\right] - \frac{2}{t^2}$$
$$+ \frac{2\lambda}{\sigma^2}\mathrm{E}_q\left[(\theta - \mu)\frac{\phi\{\lambda(\theta - m)\}}{\Phi\{\lambda(\theta - m)\}}\right].$$

S2. SGD BASED ON REPARAMETRIZATION TRICK

As $\theta = \mu + T^{-\top}z$, we have

$$d\theta = d\mu \quad \text{and} \quad d\theta = -T^{-\top}(dT^\top)T^{-\top}z.$$

Recall that

$$g(\lambda, \theta) = \nabla_\theta \log h(\theta) + TT^\top(\theta - \mu),$$
$$f(\lambda, \theta) = T^{-1}\nabla_\theta \log h(\theta) + T^\top(\theta - \mu).$$

Let vec$(\cdot)$ be the operator that stacks all elements of a matrix into a vector columnwise from left to right. In addition, let K be the commutation matrix such that $K\mathrm{vec}(A) = \mathrm{vec}(A^\top)$, and L be the elimination matrix such that $L\mathrm{vec}(A) = \mathrm{vech}(A)$ for any $d \times d$ matrix A, and $L^\top \mathrm{vech}(A) = \mathrm{vec}(A)$ if A is lower triangular.

Differentiating $g(\lambda, \theta)$ w.r.t. μ,

$$dg(\lambda, \theta) = \{\nabla_\theta^2 \log h(\theta)\}^\top d\theta + TT^\top(d\theta - d\mu)$$
$$= \{\nabla_\theta^2 \log h(\theta)\}^\top d\mu$$
$$\therefore \nabla_\mu g(\lambda, \theta) = \nabla_\theta^2 \log h(\theta).$$

Differentiating $g(\lambda, \theta)$ w.r.t. vech(T),

$$dg(\lambda, \theta) = \{\nabla_\theta^2 \log h(\theta)\}^\top d\theta + (dT)T^\top(\theta - \mu)$$
$$+ T(dT^\top)(\theta - \mu) + TT^\top(d\theta)$$
$$= -\{\nabla_\theta^2 \log h(\theta)\}^\top T^{-\top}(dT^\top)T^{-\top}z$$
$$+ (dT)T^\top(\theta - \mu) + T(dT^\top)(\theta - \mu)$$
$$- T(dT^\top)T^{-\top}z$$
$$= -\{\nabla_\theta^2 \log h(\theta)\}^\top T^{-\top}(dT^\top)T^{-\top}z + (dT)z$$
$$= \{-(z^\top T^{-1} \otimes \nabla_\theta^2 \log h(\theta)^\top T^{-\top})K$$
$$+ (z^\top \otimes I_d)\}L^\top d\mathrm{vech}(T)$$
$$= \{-(T^{-1}\nabla_\theta^2 \log h(\theta) \otimes T^{-\top}z)$$
$$+ (z \otimes I_d)\}^\top L^\top d\mathrm{vech}(T).$$

$$\therefore \nabla_{\text{vech}(T)}g(\lambda,\theta) = L\{(z \otimes I_d)$$
$$- (T^{-1}\nabla_\theta^2 \log h(\theta) \otimes T^{-\top}z)\}.$$

Differentiating $f(\lambda,\theta)$ w.r.t. μ,
$$df(\lambda,\theta) = T^{-1}\{\nabla_\theta^2 \log h(\theta)\}^\top d\theta + T^\top(d\theta - d\mu)$$
$$= T^{-1}\{\nabla_\theta^2 \log h(\theta)\}^\top d\mu.$$
$$\therefore \nabla_\mu f(\lambda,\theta) = \nabla_\theta^2 \log h(\theta)T^{-\top}.$$

Differentiating $f(\lambda,\theta)$ w.r.t. $\text{vech}(T)$,
$$df(\lambda,\theta) = -T^{-1}(dT)T^{-1}\nabla_\theta \log h(\theta) + T^\top d\theta$$
$$+ (dT^\top)(\theta - \mu) + T^{-1}\{\nabla_\theta^2 \log h(\theta)\}^\top d\theta$$
$$= -T^{-1}(dT)T^{-1}\nabla_\theta \log h(\theta) + (dT^\top)(\theta - \mu)$$
$$- T^{-1}\{\nabla_\theta^2 \log h(\theta)\}^\top T^{-\top}dT^\top T^{-\top}z$$
$$- (dT^\top)T^{-\top}z$$
$$= -\{(z^\top T^{-1} \otimes T^{-1}\nabla_\theta^2 \log h(\theta)^\top T^{-\top})K$$
$$+ (\nabla_\theta \log h(\theta)^\top T^{-\top} \otimes T^{-1})\}L^\top d\text{vech}(T)$$
$$= -\{(T^{-1}\nabla_\theta^2 \log h(\theta)T^{-\top} \otimes T^{-\top}z)$$
$$+ (T^{-1}\nabla_\theta \log h(\theta) \otimes T^{-\top})\}^\top L^\top d\text{vech}(T).$$

$$\therefore \nabla_{\text{vech}(T)}f(\lambda,\theta) = -L\{(T^{-1}\nabla_\theta^2 \log h(\theta)T^{-\top} \otimes T^{-\top}z)$$
$$+ (T^{-1}\nabla_\theta \log h(\theta) \otimes T^{-\top})\}.$$

Differentiating
$$F(\lambda) = \mathrm{E}_\phi\left\{g(\lambda,\mu + T^{-\top}z)^\top g(\lambda,\mu + T^{-\top}z)\right\}$$
with respect to μ,
$$dF(\lambda) = \mathrm{E}_\phi\left[2g(\lambda,\theta)^\top dg(\lambda,\theta)\right]$$
$$= \mathrm{E}_\phi\left[2g(\lambda,\theta)^\top\{\nabla_\theta^2 \log h(\theta)\}^\top d\mu\right].$$
$$\therefore \nabla_\mu F(\lambda) = 2\mathrm{E}_\phi\left[\{\nabla_\theta^2 \log h(\theta)\}g(\lambda,\theta)\right].$$

Next we differentiate $F(\lambda)$ with respect to $\text{vech}(T)$.
$$dF(\lambda) = \mathrm{E}_\phi\left[2g(\lambda,\theta)^\top dg(\lambda,\theta)\right]$$
$$= 2\mathrm{E}_\phi\left[g(\lambda,\theta)^\top\{-(T^{-1}\nabla_\theta^2 \log h(\theta) \otimes T^{-\top}z)$$
$$+ (z \otimes I_d)\}^\top L^\top d\text{vech}(T)\right],$$

$$\nabla_{\text{vech}(T)}F(\lambda) = 2L\mathrm{E}_\phi\left[\{-(T^{-1}\nabla_\theta^2 \log h(\theta) \otimes T^{-\top}z)\right.$$
$$+ (z \otimes I_d)\}g(\lambda,\theta)]$$
$$= 2\mathrm{E}_\phi\text{vech}\{-T^{-\top}zg(\lambda,\theta)^\top\nabla_\theta^2 \log h(\theta)T^{-\top}$$
$$+ g(\lambda,\theta)z^\top\}.$$

Differentiating $S(\lambda)$ with respect to μ,
$$dS(\lambda) = \mathrm{E}_\phi\left[\{2f(\lambda,\theta)\}^\top df(\lambda,\theta)\right]$$
$$= \mathrm{E}_\phi\left[\{2f(\lambda,\theta)\}^\top T^{-1}\{\nabla_\theta^2 \log h(\theta)\}^\top d\mu\right],$$
$$\therefore \nabla_\mu S(\lambda) = 2\mathrm{E}_\phi\{\nabla_\theta^2 \log h(\theta)T^{-T}f(\lambda,\theta)\}.$$

Differentiating $S(\lambda)$ with respect to $\text{vech}(T)$,
$$dS(\lambda) = \mathrm{E}_\phi\left[2f(\lambda,\theta)^\top df(\lambda,\theta)\right]$$
$$= -2\mathrm{E}_\phi[f(\lambda,\theta)^\top\{(T^{-1}\nabla_\theta^2 \log h(\theta)T^{-\top} \otimes T^{-\top}z)$$
$$+ (T^{-1}\nabla_\theta \log h(\theta) \otimes T^{-\top})\}^\top L^\top d\text{vech}(T)],$$

$$\nabla_{\text{vech}(T)}S(\lambda)$$
$$= -2L\mathrm{E}_\phi\left[\{(T^{-1}\nabla_\theta^2 \log h(\theta)T^{-\top} \otimes T^{-\top}z)\right.$$
$$+ (T^{-1}\nabla_\theta \log h(\theta) \otimes T^{-\top})\}f(\lambda,\theta)]$$
$$= -2\mathrm{E}_\phi\text{vech}\{T^{-\top}f(\lambda,\theta)\nabla_\theta \log h(\theta)^\top T^{-\top}$$
$$+ T^{-\top}zf(\lambda,\theta)^\top T^{-1}\nabla_\theta^2 \log h(\theta)T^{-\top}\}.$$

S2.1 Variance of gradient estimates

We have
$$g_\mu^{\text{KL}} = \nabla_\theta \log h(\theta) + Tz = -\Lambda(\theta - \nu) + Tz$$
$$= -\Lambda(T^{-\top}z + \mu - \nu) + Tz$$
$$= (T - \Lambda T^{-\top})z - \Lambda(\mu - \nu),$$
$$g_\mu^{\text{F}} = -2\nabla_\theta^2 \log h(\theta)g_\mu^{\text{KL}} = -2(-\Lambda)g_\mu^{\text{KL}} = 2\Lambda g_\mu^{\text{KL}},$$
$$g_\mu^{\text{S}} = -2\nabla_\theta^2 \log h(\theta)T^{-\top}T^{-1}g_\mu^{\text{KL}}$$
$$= 2\Lambda T^{-\top}T^{-1}g_\mu^{\text{KL}},$$
$$g_T^{\text{KL}} = T^{-\top}z(\mu - \nu)^\top\Lambda T^{-\top}$$
$$- T^{-\top}zz^\top(T^\top - T^{-1}\Lambda)T^{-\top},$$
$$g_T^{\text{F}} = 2\{\Lambda(\mu - \nu)z^\top + T^{-\top}z(\mu - \nu)^\top\Lambda^2 T^{-\top}$$
$$- (T - \Lambda T^{-\top})zz^\top$$
$$- T^{-\top}zz^\top(T^\top - T^{-1}\Lambda)\Lambda T^{-\top}\},$$

$$g_T^{\mathrm{S}} = 2[-\Sigma(T - \Lambda T^{-\top})\{zz^\top T^{-1} + z(\mu - \nu)^\top\}$$
$$\times \Lambda T^{-\top} + \Sigma\Lambda(\mu - \nu)\{z^\top T^{-1} + (\mu - \nu)^\top\}\Lambda T^{-\top}$$
$$+ T^{-\top}\{z(\mu - \nu)^\top\Lambda - zz^\top(T^\top - T^{-1}\Lambda)\}\Sigma\Lambda T^{-\top}],$$

and

$$\mathrm{Var}(g_\mu^{\mathrm{KL}}) = (T - \Lambda T^{-\top})(T^\top - T^{-1}\Lambda)$$
$$= \Sigma^{-1} - 2\Lambda + \Lambda\Sigma\Lambda,$$
$$\mathrm{Var}(g_\mu^{\mathrm{F}}) = 4\Lambda\mathrm{Var}(g_\mu^{\mathrm{KL}})\Lambda,$$
$$\mathrm{Var}(g_\mu^{\mathrm{S}}) = 4\Lambda T^{-\top}T^{-1}\mathrm{Var}(g_\mu^{\mathrm{KL}})T^{-\top}T^{-1}\Lambda.$$

To simplify the derivation of the variance with respect to T_{ii}, we further assume that both Λ and T are diagonal matrices. Under this assumption, the gradient terms can be expressed as

$$g_{T_{ii}}^{\mathrm{KL}} = \frac{\Lambda_{ii}(\mu_i - \nu_i)}{T_{ii}^2}z_i + \left(-\frac{1}{T_{ii}} + \frac{\Lambda_{ii}}{T_{ii}^3}\right)z_i^2,$$

$$g_{T_{ii}}^{\mathrm{F}} = 2\left(\Lambda_{ii} + \frac{\Lambda_{ii}^2}{T_{ii}^2}\right)(\mu_i - \nu_i)z_i + 2\left(-T_{ii} + \frac{\Lambda_{ii}^2}{T_{ii}^3}\right)z_i^2$$
$$= 2(T_{ii}^2 + \Lambda_{ii})g_{T_{ii}}^{\mathrm{KL}},$$

$$g_{T_{ii}}^{\mathrm{S}} = 2\frac{\Lambda_{ii}^2(\mu_i - \nu_i)^2}{T_{ii}^3} + 2z_i(\mu_i - \nu_i)\left(-\frac{\Lambda_{ii}}{T_{ii}^2} + 3\frac{\Lambda_{ii}^2}{T_{ii}^4}\right)$$
$$+ 4z_i^2\left(-\frac{\Lambda_{ii}}{T_{ii}^3} + \frac{\Lambda_{ii}^2}{T_{ii}^5}\right).$$

Utilizing the properties $\mathrm{Var}(z_i) = 1$, $\mathrm{Var}(z_i^2) = 2$ and $\mathrm{cov}(z_i, z_i^2) = 0$, we obtain

$$\mathrm{Var}(g_{T_{ii}}^{\mathrm{KL}}) = \frac{1}{T_{ii}^4}\left\{\Lambda_{ii}^2(\mu_i - \nu_i)^2 + 2\left(T_{ii} - \frac{\Lambda_{ii}}{T_{ii}}\right)^2\right\},$$

$$\mathrm{Var}(g_{T_{ii}}^{\mathrm{F}}) = 4(T_{ii}^2 + \Lambda_{ii})^2\mathrm{Var}(g_{T_{ii}}^{\mathrm{KL}}),$$

$$\mathrm{Var}(g_{T_{ii}}^{\mathrm{S}}) = \frac{4\Lambda_{ii}^2}{T_{ii}^8}\left\{(3\Lambda_{ii} - T_{ii}^2)^2(\mu_i - \nu_i)^2\right.$$
$$\left. + 8\left(T_{ii} - \frac{\Lambda_{ii}}{T_{ii}}\right)^2\right\}.$$

S3. SGD BASED ON BATCH APPROXIMATION

We have

$$\hat{S}_{q_t}(\lambda) = \frac{1}{B}\sum_{b=1}^{B}\{g_h(\theta_i)^\top\Sigma g_h(\theta_i) + 2g_h(\theta_i)^\top(\theta_i - \mu)$$
$$+ (\theta_i - \mu)^\top\Sigma^{-1}(\theta_i - \mu)\}$$

$$= \frac{1}{B}\sum_{b=1}^{B}[\{g_h(\theta_i) - \bar{g}_h + \bar{g}_h\}^\top\Sigma\{g_h(\theta_i) - \bar{g}_h + \bar{g}_h\}$$
$$+ 2\{g_h(\theta_i) - \bar{g}_h + \bar{g}_h\}^\top(\theta_i - \bar{\theta} + \bar{\theta} - \mu)$$
$$+ (\theta_i - \bar{\theta} + \bar{\theta} - \mu)^\top\Sigma^{-1}(\theta_i - \bar{\theta} + \bar{\theta} - \mu)]$$
$$= \mathrm{tr}\{(C_g + \bar{g}_h\bar{g}_h^\top)\Sigma\} + \mathrm{tr}(C_\theta\Sigma^{-1})$$
$$+ (\mu - \bar{\theta})^\top\Sigma^{-1}(\mu - \bar{\theta}) - 2\bar{g}_h^\top(\mu - \bar{\theta})$$
$$+ \frac{2}{B}\sum_{b=1}^{B}\{g_h(\theta_i) - \bar{g}_h\}^\top(\theta_i - \bar{\theta})$$
$$= \mathrm{tr}(V\Sigma) + \mathrm{tr}(U\Sigma^{-1}) + 2\mathrm{tr}(W),$$

$$\hat{F}_{q_t}(\lambda) = \frac{1}{B}\sum_{b=1}^{B}\{2g_h(\theta_i)^\top\Sigma^{-1}(\theta_i - \mu)$$
$$+ (\theta_i - \mu)^\top\Sigma^{-2}(\theta_i - \mu)\} + g_h(\theta_i)^\top g_h(\theta_i)$$
$$= \frac{1}{B}\sum_{b=1}^{B}[\{g_h(\theta_i) - \bar{g}_h + \bar{g}_h\}^\top\{g_h(\theta_i) - \bar{g}_h + \bar{g}_h\}$$
$$+ 2\{g_h(\theta_i) - \bar{g}_h + \bar{g}_h\}^\top\Sigma^{-1}(\theta_i - \bar{\theta} + \bar{\theta} - \mu)$$
$$+ (\theta_i - \bar{\theta} + \bar{\theta} - \mu)^\top\Sigma^{-2}(\theta_i - \bar{\theta} + \bar{\theta} - \mu)]$$
$$= \mathrm{tr}(C_g + \bar{g}_h\bar{g}_h^\top) + 2\mathrm{tr}(C_{\theta g}\Sigma^{-1}) + \mathrm{tr}(C_\theta\Sigma^{-2})$$
$$+ (\mu - \bar{\theta})^\top\Sigma^{-2}(\mu - \bar{\theta}) - 2\bar{g}_h^\top\Sigma^{-1}(\mu - \bar{\theta})$$
$$= \mathrm{tr}(V) + \mathrm{tr}(U\Sigma^{-2}) + 2\mathrm{tr}(W\Sigma^{-1}),$$

where $U = C_\theta + (\mu - \bar{\theta})(\mu - \bar{\theta})^\top$, $V = C_g + \bar{g}_h\bar{g}_h^\top$ and $W = C_{\theta g} - (\mu - \bar{\theta})\bar{g}_h^T$. Note that U and V are symmetric but W is not. Differentiating with respect to μ and T,

$$\nabla_\mu\hat{S}_{q_t}(\lambda) = 2\Sigma^{-1}(\mu - \bar{\theta}) - 2\bar{g}_h.$$
$$d\hat{S}_{q_t}(\lambda) = d\{\mathrm{tr}(VT^{-\top}T^{-1}) + \mathrm{tr}(UTT^\top)\}$$
$$= -\mathrm{tr}(VT^{-\top}dT^\top\Sigma) - \mathrm{tr}(V\Sigma dTT^{-1})$$
$$+ \mathrm{tr}(UdTT^\top) + \mathrm{tr}(UTdT^\top)$$
$$= \mathrm{tr}\{(UT - \Sigma VT^{-\top})dT^\top\}$$
$$+ \mathrm{tr}\{(T^\top U - T^{-1}V\Sigma)dT\}$$
$$= 2\mathrm{vec}(UT - \Sigma VT^{-\top})^\top L^\top d\mathrm{vech}(T).$$

$$\nabla_{\mathrm{vech}(T)}\hat{S}_{q_t}(\lambda) = 2\mathrm{vech}(UT - \Sigma VT^{-\top}).$$
$$\nabla_\mu\hat{F}_{q_t}(\lambda) = \Sigma^{-1}\nabla_\mu\hat{S}_{q_t}(\lambda).$$
$$d\hat{F}_{q_t}(\lambda) = d\{\mathrm{tr}(UTT^\top TT^\top) + 2\mathrm{tr}(WTT^\top)\}$$

$$= \text{tr}(U dT T^\top \Sigma^{-1}) + \text{tr}(UT dT^\top \Sigma^{-1})$$
$$+ \text{tr}(U\Sigma^{-1} dT T^\top) + \text{tr}(U\Sigma^{-1} T dT^\top)$$
$$+ 2\text{tr}(W dT T^\top) + 2\text{tr}(WT dT^\top)$$
$$= \text{tr}\{(T^\top \Sigma^{-1} U + T^\top U \Sigma^{-1}) dT\}$$
$$+ \text{tr}\{(\Sigma^{-1} UT + U\Sigma^{-1} T) dT^\top\}$$
$$+ 2\text{tr}(T^\top W dT) + 2\text{tr}(WT dT^\top)$$
$$= 2\text{vec}(\Sigma^{-1} UT + U\Sigma^{-1} T + W^\top T$$
$$+ WT)^\top L^\top d\text{vech}(T).$$
$$\nabla_{\text{vech}(T)} \hat{F}_{q_t}(\lambda) = 2\text{vech}\{(W + W^\top + \Sigma^{-1} U$$
$$+ U\Sigma^{-1})T\}.$$

S4. GRADIENTS FOR GLMMS

Let $X_i = (X_{i1}, \ldots, X_{in_i})^\top$ and $Z_i = (Z_{i1}, \ldots, Z_{in_i})^\top$ be design matrices for the ith subject. Recall that $b_i \sim N(0, G^{-1})$, $G = WW^\top$, W^* is such that $W_{ii}^* = \log(W_{ii})$ and $W_{ij}^* = W_{ij}$ if $i \neq j$, and $\zeta = \text{vech}(W^*)$. Let J^W be an $r \times r$ matrix with diagonal given by $\text{diag}(W)$ and all off-diagonal entries being 1, and $D^W = \text{diag}\{\text{vech}(J^W)\}$. Then $d\text{vech}(W) = D^W d\text{vech}(W^*)$. We have

$$\nabla_\theta \log h(\theta) = [\nabla_{b_1} \log h(\theta)^\top, \ldots, \nabla_{b_n} \log h(\theta)^\top,$$
$$\nabla_\beta \log h(\theta)^\top, \nabla_\zeta \log h(\theta)^\top]^\top,$$

where

$$\nabla_{b_i} \log h(\theta) = \sum_{j=1}^{n_i} \{y_{ij} - A'(\eta_{ij})\} Z_{ij} - Gb_i,$$

$$\nabla_\beta \log h(\theta) = \sum_{i=1}^{n} \sum_{j=1}^{n_i} \{y_{ij} - A'(\eta_{ij})\} X_{ij} - \frac{\beta}{\sigma_\beta^2},$$

$$\nabla_\zeta \log h(\theta) = -D^W \text{vech}(\widetilde{W}) + n\text{vech}(I_r) - \frac{\zeta}{\sigma_\zeta^2},$$

and $\widetilde{W} = \sum_{i=1}^{n} b_i b_i^\top W$. For the hessian $\nabla_\theta^2 \log h(\theta)$,

$$\nabla_{b_i, \eta}^2 \log h(\theta) = \begin{bmatrix} \nabla_{b_i, \beta}^2 \log h(\theta) \\ \nabla_{b_i, \zeta}^2 \log h(\theta) \end{bmatrix},$$

$$\nabla_\eta^2 \log h(\theta) = \begin{bmatrix} \nabla_\beta^2 \log h(\theta) & 0 \\ 0 & \nabla_\zeta^2 \log h(\theta) \end{bmatrix}.$$

Let $B_i = \text{diag}([A''(\eta_{i1}), \ldots, A''(\eta_{in_i})]^\top)$. The second order derivatives of $\log h(\theta)$ are

$$\nabla_{b_i}^2 \log h(\theta) = -(Z_i^\top B_i Z_i + G), \text{ for },$$

$$\nabla_\beta^2 \log h(\theta) = -\left(\sum_{i=1}^{n} X_i^\top B_i X_i + \frac{1}{\sigma_\beta^2} I_p\right),$$

$$\nabla_\zeta^2 \log h(\theta) = -S - D^W L \sum_{i=1}^{n} (I_r \otimes b_i b_i^\top) L^\top D^W$$
$$- \frac{1}{\sigma_\zeta^2} I_{r(r+1)/2},$$

$$\nabla_{\beta, b_i}^2 \log h(\theta) = -X_i^\top B_i Z_i,$$

$$\nabla_{\zeta, b_i}^2 \log h(\theta) = -D^W L(W^\top b_i \otimes I_r + W^\top \otimes b_i),$$

where $S = \text{diag}[\text{vech}\{\text{dg}(W)\text{dg}(\widetilde{W})\}]$ and $\text{dg}(A)$ is a copy of A with all off-diagonal entries set to 0.

The derivations for $\nabla_{b_i}^2 \log h(\theta)$, $\nabla_\beta^2 \log h(\theta)$ and $\nabla_{b_i, \beta}^2 \log h(\theta)$ are straightforward. More details for $\nabla_{\zeta^2}^2 \log h(\theta)$ and $\nabla_{b_i, \zeta}^2 \log h(\theta)$ are given below. Differentiating $\nabla_\zeta \log h(\theta)$ w.r.t. b_i, we have

$$d\nabla_\zeta \log h(\theta) = -D^W \sum_{i=1}^{n} \text{vech}\{(db_i) b_i^\top W + b_i (db_i^\top) W\}$$
$$= -D^W L \sum_{i=1}^{n} [(W^\top b_i \otimes I_r) + (W^\top \otimes b_i)] db_i.$$

Differentiating $\nabla_\zeta \log h(\theta)$ w.r.t. ζ, we have

$$d\nabla_\zeta \log h(\theta) = -(dD^W) \sum_{i=1}^{n} \text{vech}(b_i b_i^\top W)$$
$$- D^W \sum_{i=1}^{n} \text{vech}\{b_i b_i^\top (dW)\} - \frac{1}{\sigma_\zeta^2} d\zeta$$
$$= -D^W L \sum_{i=1}^{n} (I_r \otimes b_i b_i^\top) d\text{vec}(W)$$
$$- Sd\zeta - \frac{1}{\sigma_\zeta^2} d\zeta$$
$$= -D^W L \sum_{i=1}^{n} (I_r \otimes b_i b_i^\top) L^T D^W d\zeta$$
$$- Sd\zeta - \frac{1}{\sigma_\zeta^2} d\zeta.$$

S5. GRADIENTS FOR STOCHASTIC VOLATILITY MODEL

For this model, the gradients of $\log h(\theta)$ are,

$$\nabla_{b_1} \log h(\theta) = -(1-\phi^2)b_1 + \phi(b_2 - \phi b_1) - \frac{e^\alpha}{2}$$
$$+ \frac{e^\alpha y_1^2}{2} \exp(-\lambda - e^\alpha b_1),$$

$$\nabla_{b_t} \log h(\theta) = \phi(b_{t+1} - \phi b_t) - (b_t - \phi b_{t-1}) - \frac{e^\alpha}{2}$$
$$+ \frac{e^\alpha}{2} y_t^2 \exp(-\lambda - e^\alpha b_t) \text{ for } 1 < t < n,$$

$$\nabla_{b_n} \log h(\theta) = -(b_n - \phi b_{n-1}) - \frac{e^\alpha}{2}$$
$$+ \frac{e^\alpha}{2} y_n^2 \exp(-\lambda - e^\alpha b_n),$$

$$\nabla_\alpha \log h(\theta) = \frac{1}{2} \sum_{t=1}^{n} y_t^2 b_t \exp(\alpha - \lambda - e^\alpha b_t)$$
$$- \frac{e^\alpha}{2} \sum_{t=1}^{n} b_t - \frac{\alpha}{\sigma_0^2},$$

$$\nabla_\lambda \log h(\theta) = -\frac{n}{2} + \frac{1}{2} \sum_{t=1}^{n} y_t^2 \exp(-\lambda - e^\alpha b_t) - \frac{\lambda}{\sigma_0^2},$$

$$\nabla_\psi \log h(\theta) = \left\{ \phi b_1^2 - \frac{\phi}{(1-\phi^2)} + \sum_{t=1}^{n-1} (b_{t+1} - \phi b_t) b_t \right\}$$
$$\times \frac{e^\psi}{(e^\psi + 1)^2} - \frac{\psi}{\sigma_0^2}.$$

$$\nabla_{b_n,\psi}^2 \log h(\theta) = \frac{e^\psi b_{n-1}}{(e^\psi + 1)^2},$$

$$\nabla_\alpha^2 \log h(\theta) = \frac{1}{2} \sum_{t=1}^{n} y_t^2 b_t \exp\{\alpha - \lambda - e^\alpha b_t\}(1 - e^\alpha b_t)$$
$$- \frac{e^\alpha}{2} \sum_{t=1}^{n} b_t - \frac{1}{\sigma_0^2},$$

$$\nabla_\lambda^2 \log h(\theta) = -\frac{1}{2} \sum_{t=1}^{n} y_t^2 \exp(-\lambda - e^\alpha b_t) - \frac{1}{\sigma_0^2},$$

$$\nabla_\psi^2 \log h(\theta) = \left\{ b_1^2 - \sum_{t=1}^{n-1} b_t^2 - \frac{1+\phi^2}{(1-\phi^2)^2} \right\} \frac{e^{2\psi}}{(e^\psi + 1)^4}$$
$$+ \left\{ \phi b_1^2 - \frac{\phi}{(1-\phi^2)} + \sum_{t=1}^{n-1} (b_{t+1} - \phi b_t) b_t \right\}$$
$$\times \frac{e^\psi(1 - e^\psi)}{(e^\psi + 1)^3} - \frac{1}{\sigma_0^2},$$

$$\nabla_{\alpha,\lambda}^2 \log h(\theta) = -\frac{1}{2} \sum_{t=1}^{n} y_t^2 b_t \exp\{\alpha - \lambda - e^\alpha b_t\},$$

$$\nabla_{\psi,\lambda}^2 \log h(\theta) = \nabla_{\psi,\alpha}^2 \log h(\theta) = 0.$$

The second order derivatives of $\log h(\theta)$ are,

$$\nabla_{b_1}^2 \log h(\theta) = -1 - \frac{y_1^2}{2} \exp\{2\alpha - \lambda - e^\alpha b_1\},$$

$$\nabla_{b_t}^2 \log h(\theta) = -\phi^2 - 1 - y_t^2 \exp\{2\alpha - \lambda - e^\alpha b_t\}/2,$$

$$\nabla_{b_n}^2 \log h(\theta) = -1 - y_n^2 \exp\{2\alpha - \lambda - e^\alpha b_n\}/2,$$

$$\nabla_{b_i,b_j}^2 \log h(\theta) = \phi \mathbb{1}_{|i-j|=1},$$

$$\nabla_{b_t,\alpha}^2 \log h(\theta) = \frac{y_t^2}{2} \exp\{\alpha - \lambda - e^\alpha b_t\}(1 - b_t e^\alpha) - \frac{e^\alpha}{2},$$

$$\nabla_{b_t,\lambda}^2 \log h(\theta) = -y_t^2 \exp\{\alpha - \lambda - e^\alpha b_t\}/2$$

$$\nabla_{b_1,\psi}^2 \log h(\theta) = \frac{b_2 e^\psi}{(e^\psi + 1)^2},$$

$$\nabla_{b_t,\psi}^2 \log h(\theta) = \frac{e^\psi(b_{t+1} - 2\phi b_t + b_{t-1})}{(e^\psi + 1)^2},$$